nature chemical biology

ARTICLE

PUBLISHED ONLINE: 27 NOVEMBER 2011 | DOI: 10.1038/NCHEMBIO.721

Eukaryotic DNA polymerases require an iron-sulfur cluster for the formation of active complexes

Daili J A Netz[1], Carrie M Stith[2], Martin Stümpfig[1], Gabriele Köpf[1], Daniel Vogel[1], Heide M Genau[1], Joseph L Stodola[2], Roland Lill[1]*, Peter M J Burgers[2]* & Antonio J Pierik[1]*

The eukaryotic replicative DNA polymerases (Pol α, δ and ε) and the major DNA mutagenesis enzyme Pol ζ contain two conserved cysteine-rich metal-binding motifs (CysA and CysB) in the C-terminal domain (CTD) of their catalytic subunits. Here we demonstrate by *in vivo* and *in vitro* approaches the presence of an essential [4Fe-4S] cluster in the CysB motif of all four yeast B-family DNA polymerases. Loss of the [4Fe-4S] cofactor by cysteine ligand mutagenesis in Pol3 destabilized the CTD and abrogated interaction with the Pol31 and Pol32 subunits. Reciprocally, overexpression of accessory subunits increased the amount of the CTD-bound Fe-S cluster. This implies an important physiological role of the Fe-S cluster in polymerase complex stabilization. Further, we demonstrate that the Zn-binding CysA motif is required for PCNA-mediated Pol δ processivity. Together, our findings show that the function of eukaryotic replicative DNA polymerases crucially depends on different metallocenters for accessory subunit recruitment and replisome stability.

Replication of double-stranded nuclear DNA in eukaryotes is performed through the coordinated work of three DNA polymerase complexes, Pol α, Pol δ and Pol ε (ref. 1). Pol α together with the primase complex initiates the synthesis of short RNA primers, which are subsequently extended by Pol δ and Pol ε for processive synthesis of the lagging and leading strands, respectively[2,3]. In *Saccharomyces cerevisiae,* Pol α has four subunits (Pol1, Pol12, Pri1, Pri2), Pol δ has three (Pol3, Pol31, Pol32) and Pol ε has four (Pol2, Dpb2, Dpb3 and Dpb4). The catalytic subunits Pol1, Pol2 and Pol3 are phylogenetically related and belong to the class B DNA polymerases[4]. They are tightly associated with the so-called B subunits Pol12, Dpb2 and Pol31, respectively. The B subunits are all essential and share both phosphodiesterase-like and oligosaccharide-binding domains[5,6]. Eukaryotes contain a fourth class B DNA polymerase, Pol ζ, which is the major enzyme responsible for mutagenesis in response to DNA damage[7,8]. Pol ζ, composed of the catalytic subunit Rev3 and the accessory subunit Rev7, is not essential for growth in yeast, but disruption of *REV3L* in mice causes embryonic lethality[9].

Eight conserved cysteine residues are present in the CTD of all four eukaryotic class B DNA polymerases (**Supplementary Results**, **Supplementary Fig. 1**). This domain is absent in the other classes of DNA polymerases such as bacterial or mitochondrial DNA polymerases. The first set of four cysteine residues (CysA) resembles a zinc ribbon motif ($C\text{-}X_2\text{-}C\text{-}X_{7-31}\text{-}C\text{-}X_2\text{-}C$)[10], whereas the C-terminal set (CysB) has an atypical pattern. This CTD is not present in B-family DNA polymerases of bacteriophages, herpes viruses, proteobacteria and archaea. However, phylogenetic analysis has indicated that a motif similar to CysB is present in the CTD of euryarchaeal D-family polymerases[11]. The crystal structure of the yeast class B Pol3 has been determined, yet it lacks the entire CTD as full-length Pol3 isolated from yeast is prone to aggregation[12]. Two three-dimensional structures of the CTD of DNA polymerase α have been reported. A Zn^{2+}-reconstituted synthetic oligopeptide corresponding to the CysB region of human Pol1 was structurally characterized by NMR spectroscopy[13]. Recently, the crystal structure of the yeast Pol1-CTD in complex with Pol12 was reported[14]. This complex was purified from *Escherichia coli* after heterologous expression, and it contains a Zn^{2+} ion in both the CysA and CysB motifs. This study provided structural information for earlier biochemical studies, which had described interactions between the CTDs and their corresponding B-subunits[15–17].

Intriguingly, the *pol3-13* allele of yeast, in which the second cysteine of CysB (C1074) in Pol3 is mutated to serine, is synthetically lethal with mutations in the essential genes *NBP35*, *DRE2* and *TAH18* (ref. 18). These genes encode components of the cytosolic Fe-S protein assembly (CIA) machinery, which is required for maturation of most cytosolic and nuclear Fe-S proteins[19–22]. Nbp35 together with Cfd1 serves as a scaffold complex that assembles a transiently bound Fe-S cluster in an early step of the biosynthesis process[23,24]. Dre2, an Fe-S protein, and the diflavin reductase Tah18 form an electron transfer chain using NADPH for Tah18-dependent reduction of one of the two Fe-S clusters of Dre2 (ref. 22). CIA components acting later in biogenesis encompass the Fe-only hydrogenase-like Nar1 and the β-propeller protein Cia1[25,26]. Remarkably, the CIA machinery requires a sulfur-containing compound exported by mitochondria after synthesis by the cysteine desulfurase complex Nfs1–Isd11 and other components of the mitochondrial Fe-S cluster (ISC) assembly machinery[19,27].

Although it is widely believed that both CysA and CysB of Pol3 bind Zn^{2+} ions, the synthetic lethality resulting from the combination of the *pol3-13* allele and mutations in CIA components pointed to the presence of a hitherto unrecognized Fe-S cluster in Pol3. We therefore addressed the question of whether the CTD of polymerases coordinate an Fe-S cluster and what the physiological role of such a cofactor might be. We provide *in vivo* and *in vitro* evidence that a [4Fe-4S] cluster rather than Zn^{2+} is bound to the CysB motif in all yeast B-family DNA polymerases. Assembly of this essential Fe-S cluster was strictly dependent on the function of mitochondrial Nfs1 and cytosolic Nbp35, explaining the synthetic lethality of the *pol3-13* allele and Fe-S biosynthetic genes[18]. The findings also indicate a so-far-unknown dependence of nuclear DNA synthesis on mitochondrial function. Finally, our study reveals the physiological importance of the two different metal cofactors, the [4Fe-4S]

[1]Institut für Zytobiologie und Zytopathologie, Philipps-Universität Marburg, Marburg, Germany. [2]Department of Biochemistry and Molecular Biophysics, Washington University School of Medicine, St. Louis, Missouri, USA. *e-mail: lill@staff.uni-marburg.de, burgers@biochem.wustl.edu or pierik@staff.uni-marburg.de

cluster in CysB and Zn^{2+} in CysA, in the stabilization of DNA polymerase interactions with different accessory proteins essential for processive DNA synthesis at the replication fork.

RESULTS

Eukaryotic DNA polymerases bind an Fe-S cluster *in vivo*

To investigate the presumed presence of Fe-S clusters in eukaryotic DNA polymerases, we used a sensitive *in vivo* radiolabeling assay, which measures the incorporation of ^{55}Fe into newly synthesized proteins in baker's yeast. The coding information for a C-terminal Myc tag was fused by chromosomal integration to Pol1, Pol2, Pol3 and Rev3, the catalytic subunits of the Pol α, Pol ε, Pol δ and Pol ζ complexes, respectively. No negative effects on cell growth were caused by introducing these tags. A significant ($P < 0.05$) amount of ^{55}Fe was associated with Pol1, Pol2 and Pol3 immunoprecipitated with Myc-specific beads (1.01 ± 0.19 pmol, 1.34 ± 0.17 pmol and 2.6 ± 0.2 pmol per gram of cells above respective control levels; **Fig. 1a** and **Supplementary Fig. 2**). The radiolabeling was not due to adventitious binding of iron to cysteine-rich proteins, as negligible amounts of ^{55}Fe bound to transcription factor IIIA (TFIIIA), which contains nine conserved zinc fingers (**Fig. 1a**). The presence of Fe-S clusters rather than other forms of iron was tested by measuring the dependence of ^{55}Fe binding on the mitochondrial and cytosolic Fe-S protein assembly machineries. Depletion of the cysteine desulfurase Nfs1(refs. 19,27) of the galactose-regulatable strain Gal-NFS1 by growth on glucose almost completely abolished ^{55}Fe binding to the polymerases. Proper assembly of the ^{55}Fe-S cluster requires mitochondria-localized Nfs1 because a cytosolic version of Nfs1 fails to support radiolabeling of Pol3 (**Supplementary Fig. 3**). Similarly, depletion of the CIA machinery components Nbp35 and Nar1 in regulatable yeast strains (Gal-NBP35 (ref. 20) and Gal-NAR1 (ref. 25)) abrogates Fe-S cluster formation on the polymerases (**Fig. 1a** and **Supplementary Figs. 2,4**). As Pol1 is associated with primase, which contains a [4Fe-4S] cluster in its Pri2 subunit[28], we examined the Pri2 contribution to the binding of ^{55}Fe to Pol1. Although the amount of ^{55}Fe copurified with hemagglutinin (HA)-tagged Pri2 (1.12 ± 0.28 pmol ^{55}Fe per gram of cells) was similar to that measured in Pol1-Myc (1.01 ± 0.19 pmol ^{55}Fe per gram of cells), only 20% of HA-Pri2 immunoprecipitated together with Pol1-Myc and vice versa (**Supplementary Fig. 5**). Thus, a major contribution from Pri2 to Pol1-associated ^{55}Fe radioactivity could be excluded. A similar reservation does not hold for Pol δ or Pol ε. None of the small subunits of Pol ε have conserved cysteine residues that can serve as potential ligands for an Fe-S cluster. Structural studies of the small subunits of Pol δ do not indicate the presence of potential metal binding sites[6]. Taken together, our data clearly suggest the presence of a hitherto unrecognized Fe-S cluster in all three replicative DNA polymerases *in vivo*.

The CTD of the catalytic subunit binds the Fe-S cluster

We next tested whether the Fe-S cluster is associated with the CTD, as suggested by the synthetic lethality of the *pol3-13* allele[18] and the strict conservation of the cysteine residues. As Pol3 is an essential gene and episomal copies of full-length polymerases have deleterious effects on cell growth[29], we expressed only the CTD of Pol3 (residues 982–1097) with an N-terminal HA epitope tag from a plasmid. HA–Pol3-CTD bound significant ($P < 0.05$) amounts of ^{55}Fe (4.1 ± 0.9 pmol g^{-1}; **Fig. 1b** and **Supplementary Fig. 6**), which dropped to background values in both Nfs1- and Nbp35-depleted cells. This behavior closely resembles that of full-length Pol3 (**Fig. 1a**). As no significant ($P > 0.05$) ^{55}Fe binding to full-length Rev3 could be detected, apparently because of Rev3's low abundance (**Supplementary Fig. 7**), we examined ^{55}Fe binding to HA-tagged Rev3-CTD (residues 1374–1504). In this case, a significant ($P < 0.05$) amount of ^{55}Fe (0.9 ± 0.3 pmol g^{-1}) was detected, which dropped to background values upon Nfs1 and Nbp35 depletion (**Fig. 1b**). These results provide evidence that *in vivo*, all yeast class B DNA polymerases bind Fe-S clusters in their CTD. Considering the high amino acid sequence conservation of the CTDs of all eukaryotic B-class polymerases[11] (**Supplementary Fig. 1**), we anticipate that the presence of an Fe-S cluster in polymerase CTDs extends to all eukaryotes, including humans.

Accessory subunits stabilize the Fe-S cluster in CysB

To identify which of the eight conserved cysteine residues of the polymerase CTDs are responsible for Fe-S cluster coordination, we used Pol3 as a prototype polymerase and introduced cysteine-to-alanine substitutions. In principle, the CysA and CysB motifs may independently bind an Fe-S cluster, as the corresponding segments are structurally well separated (47-Å Zn-Zn distance) by a three-helix bundle in the zinc-bound form of Pol1-CTD[14]. All cysteine residues of CysB are required for Fe-S cluster binding *in vivo* because their substitution by alanine completely abolishes ^{55}Fe incorporation into Pol3-CTD (**Fig. 2a**, right). In contrast, the amount of ^{55}Fe binding was significantly ($P < 0.05$) above background values for all cysteine-to-alanine exchanges in CysA, suggesting that some Fe-S cluster may remain bound to CysB (**Fig. 2a**, left). The weakened Fe-S cluster binding efficiency of CysA mutant proteins could be caused by a lack of polymerase complex stabilization by Pol31, even though this subunit interacts primarily with the CysB region[17].

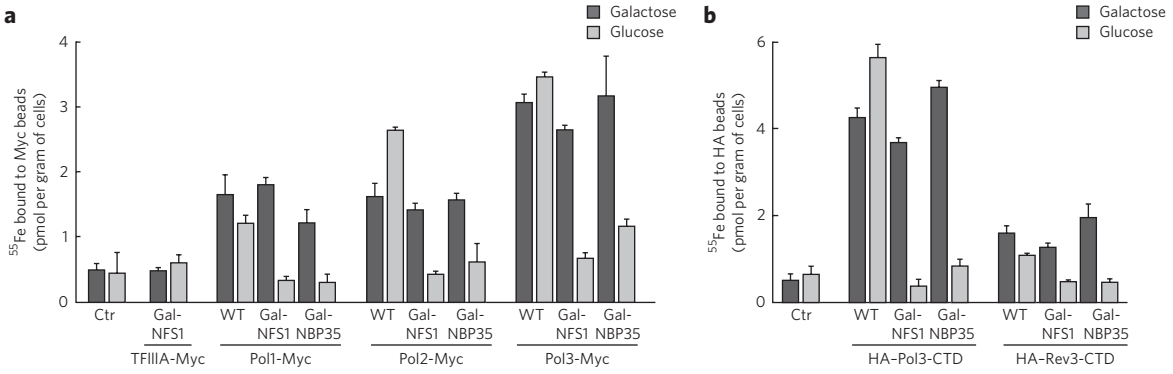

Figure 1 | Yeast replicative DNA polymerases and Rev3 contain Fe-S clusters *in vivo*. (**a**) Wild-type (WT), Gal-NFS1 or Gal-NBP35 cells harboring genomically Myc-tagged Pol1, Pol2 and Pol3 were grown in galactose- or glucose-containing medium to induce or repress, respectively, production of Nfs1 or Nbp35. After ^{55}Fe radiolabeling of cells, polymerases were immunoprecipitated from cell extracts, and bound ^{55}Fe was quantified by scintillation counting. TFIIIA-Myc expressed in Gal-NFS1 and WT cells without tagged polymerases (Ctr) served as controls. (**b**) ^{55}Fe incorporation into plasmid-encoded HA–Pol3-CTD and HA–Rev3-CTD as in **a**. Western blots for the cell extracts are presented in **Supplementary Figures 2** and **6** for **a** and **b**, respectively. Error bars, s.d. ($n \geq 3$).

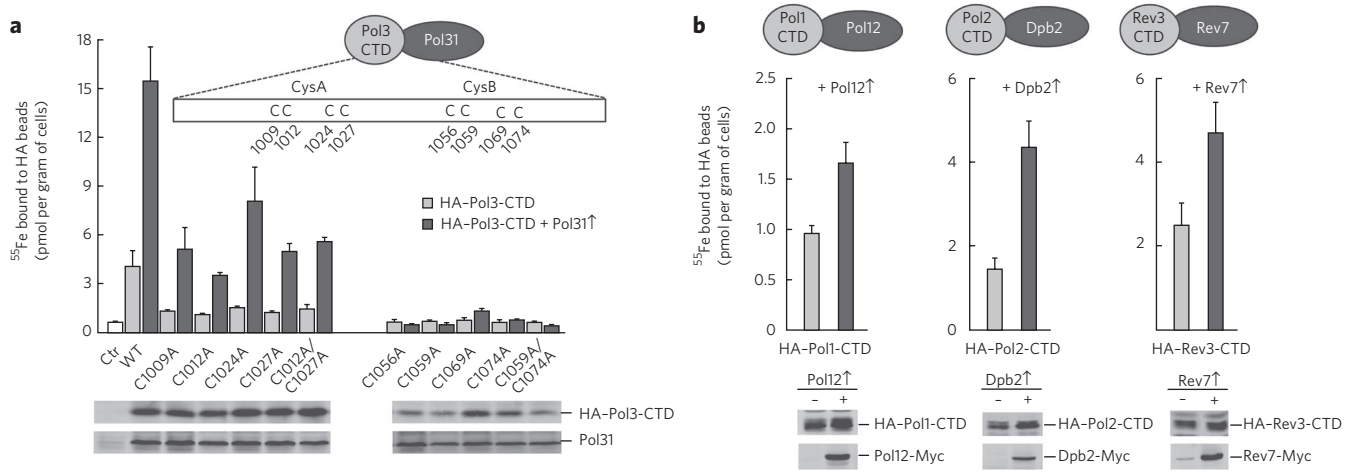

Figure 2 | The Fe-S cluster is coordinated by the CysB motif and is stabilized by accessory-subunit binding . (**a**) ^{55}Fe incorporation into plasmid-encoded HA–Pol3-CTD and cysteine-to-alanine substitutions thereof (cartoon), with (Pol31↑) or without Pol31 overexpression in wild-type yeast cells grown in galactose-containing medium. Western blots are for cell extracts with Pol31 overexpression. (**b**) ^{55}Fe incorporation into indicated plasmid-encoded polymerase CTDs, with (↑) or without overexpression of the accessory subunits (cartoon) in wild-type yeast cells grown in galactose-containing medium. Western blots are shown for indicated cell extracts. Full-length blots are presented in **Supplementary Figure 8**. Error bars, s.d. ($n \geq 3$).

Indeed, overexpression of Pol31 resulted in a four- to eight-fold higher ^{55}Fe binding to both wild-type and CysA mutant Pol3-CTDs (**Fig. 2a** and **Supplementary Fig. 8**) but not to CysB mutant proteins. Nevertheless, the greater abundance of Pol31 could not completely compensate for the Fe-S cluster binding deficit caused by cysteine exchanges in CysA. We attribute the lower ^{55}Fe content of the CysA mutant proteins to an indirect effect of the disruption of CysA motif structure due to the lack of zinc binding. This may affect the efficiency of Fe-S cluster formation in CysB. The decreased amount of protein of the CysB-mutated CTD found in immunostains of cell extracts, even upon Pol31 overexpression (**Supplementary Fig. 8a**,**c**), can be explained by the absence of the Fe-S cluster in CysB. This absence renders the protein sensitive to degradation, as frequently seen for Fe-S proteins. Together, these findings imply that only CysB is responsible for Fe-S cluster binding, whereas CysA may bind zinc[14]. We infer that Pol3–Pol31 complex formation is intrinsically linked to the presence of an intact Fe-S cluster, explaining its physiological importance for Pol δ function.

Next, we tested whether the functional connection between the presence of an Fe-S cluster on the DNA polymerase and its interaction with the respective accessory subunits also holds for the other class B family members. Overexpression of Pol12, Dpb2 and Rev7 with the CTDs of Pol1, Pol2 and Rev3, respectively, significantly ($P < 0.05$) increased the amounts of ^{55}Fe coisolated in the absence of the overproduced accessory subunits (**Fig. 2b**). Thus, the increase in the efficiency of Fe-S cluster binding to the polymerase CTDs by the respective accessory subunits appears to extend to all members of the class B family, suggesting a stabilization of Fe-S cluster binding by these subunits and vice versa.

The [4Fe-4S] cluster is required for complex formation

To characterize the type and stoichiometry of Fe-S cluster binding to DNA polymerases, we performed biochemical and spectroscopic studies. Expression of the yeast Pol1-, Pol2-, Pol3- and Rev3-CTD in *E. coli* resulted in the formation of dark inclusion bodies, which gave brownish solutions upon treatment with chaotropic agents (**Fig. 3a**). Soluble brown Pol2-, Pol3- and Rev3-CTDs could be obtained in the absence of chaotropic agents after modifications of the protocol (**Supplementary Fig. 9**). Pol1-CTD and Pol2-CTD were aggregation prone. A low yield of Pol1-CTD holoform was obtained (~0.1 Fe and S per monomer; **Supplementary Fig. 10**). This apparent lability of Fe-S cluster binding to purified Pol1-CTD may have precluded its earlier discovery in structural studies[14]. The other CTDs contained 2.0–2.6 mol non-heme iron and acid-labile sulfide per CTD, and their UV-visible (UV-vis) spectra showed a broad absorption maximum centered at 400 nm, indicative of [4Fe-4S]

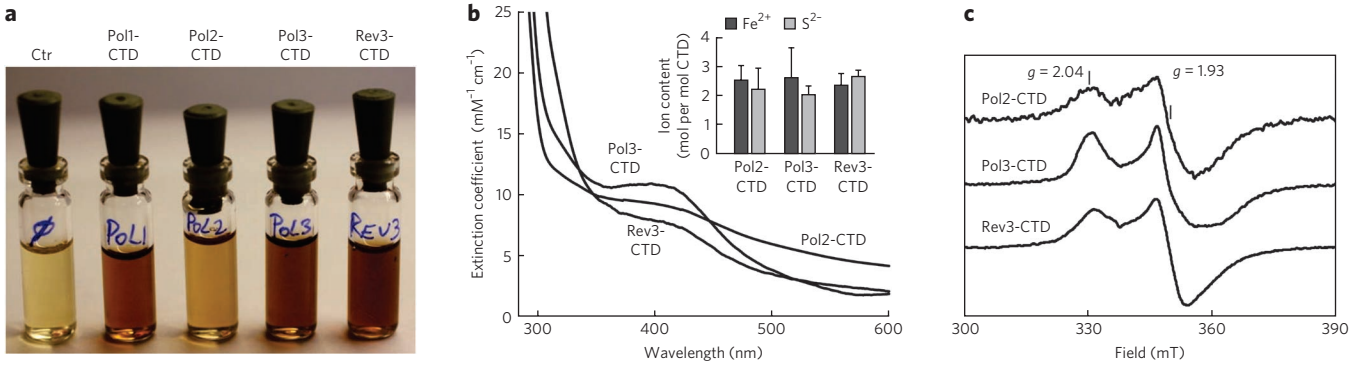

Figure 3 | Recombinant purified CTDs of Pol1, Pol2, Pol3 and Rev3 harbor a [4Fe-4S] cluster. (**a**) Solubilized inclusion bodies of indicated CTDs obtained after expression in *E. coli*. (**b**) UV-vis and (**c**) X-band EPR spectra of purified soluble Pol2-, Pol3- and Rev3-CTDs in absence of chaotropic agents. The inset in **b** shows non-heme iron and acid-labile sulfide contents. Error bars, s.d. ($n \geq 3$). Samples in **c** were reduced with 2 mM sodium dithionite (2 min). EPR conditions: 9.458 GHz, 10 K and 2 mW microwave power.

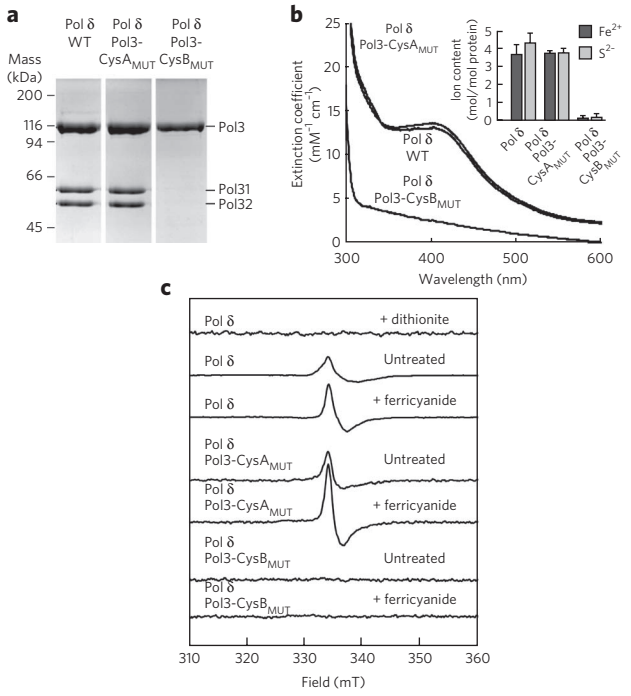

Figure 4 | Functional integrity of purified Pol δ complex depends on binding of an Fe-S cluster to Pol3. (**a**–**c**) Pol δ complex purified from yeast coexpressing wild-type (WT), CysA$_{MUT}$ (C1012S C1027S) or CysB$_{MUT}$ (C1059S C1074S) Pol3 with Pol31 and Pol32 was analyzed by (**a**) Coomassie blue–stained SDS-PAGE (**b**) UV-vis spectroscopy and chemical analysis (inset) or (**c**) EPR spectroscopy. EPR conditions and treatments with ferricyanide (2 mM) or dithionite are as in **Figure 3c**. The full-length gel for **a** is presented in **Supplementary Figure 11c**. Error bars, s.d. ($n \geq 3$).

clusters (**Fig. 3b**). These soluble CTDs did not show electron paramagnetic resonance (EPR) signals, even after oxidation with ferricyanide, excluding the presence of [3Fe-4S] clusters[30]. However, upon reduction with dithionite, EPR signals with $g = 2.04$ and $g = 1.93$ characteristic of $[4Fe\text{-}4S]^{1+}$ clusters were detected (**Fig. 3c**). Together, these results provide evidence for a single $[4Fe\text{-}4S]^{2+}$ cluster bound to the purified CTDs.

As no Fe-S cluster has been detected in any isolated DNA polymerase complex, we investigated the native Pol δ complex for such a metal center after its expression was induced and it was purified from *S. cerevisiae* (**Supplementary Fig. 11a**,**b**). Isolated Pol δ was olive yellow and contained Pol3, Pol31 and Pol32 in stoichiometric ratios (**Fig. 4a** and **Supplementary Fig. 11c**). UV-vis spectroscopy of Pol δ showed broad absorption in the 400-nm region, and chemical analysis detected approximately 4 mol of non-heme iron and acid-labile sulfide ions per mol of Pol δ (**Fig. 4b**, inset). Thus, the Fe-S content, the UV-vis spectrum and the extinction coefficient of 13 $mM^{-1}cm^{-1}$ at 400 nm indicate the presence of a single $[4Fe\text{-}4S]^{2+}$ or a single $[3Fe\text{-}4S]^{1+}$ cluster in purified Pol δ complex (**Fig. 4b**). EPR spectroscopy showed a weak signal centered at $g = 2.02$, characteristic of $[3Fe\text{-}4S]^{1+}$ clusters. Spin quantification of the EPR signal, however, accounted for only 5 ± 1% of the total Fe-S cluster content (**Fig. 4c**). This signal increased two-fold upon oxidation with ferricyanide, corresponding to just 10 ± 2% of the Fe-S cluster content. After dithionite treatment of the wild-type Pol δ complex, the $[3Fe\text{-}4S]^{1+}$ cluster EPR signal at $g = 2.02$ disappeared because of reduction to the EPR-silent $[3Fe\text{-}4S]^{0}$ state. However, native Pol δ treated with dithionite did not show a $[4Fe\text{-}4S]^{1+}$ EPR signal (**Fig. 4c**, top trace). These findings are in contrast to the results for the soluble CTDs, in which the $[4Fe\text{-}4S]^{2+}$ cluster may be reduced to the $[4Fe\text{-}4S]^{1+}$ form. The absence of an EPR signal in dithionite-treated polymerase δ could be explained by the lower redox potential of the $[4Fe\text{-}4S]^{2+}$ cluster in the intact complex in comparison to that of Pol3-CTD. Dithionite can only reduce the cluster if the midpoint potential is above −500 mV, which is apparently the case for the CTDs. Alternatively, the $[4Fe\text{-}4S]^{1+}$ cluster may have a high spin state with an EPR spectrum too broad to be detectable. A third explanation would be conversion of the $[4Fe\text{-}4S]^{1+}$ cluster to the EPR silent $[3Fe\text{-}4S]^{0}$ form. Breakdown of the cluster upon dithionite treatment is unlikely as processivity remained unaltered. Many other $[4Fe\text{-}4S]^{2+}$ cluster-containing proteins have EPR and redox properties similar to those of native Pol δ. For example, aconitase has a labile $[4Fe\text{-}4S]^{2+}$ cluster that is converted to the $[3Fe\text{-}4S]^{1+}$ form during isolation[31], and the $[4Fe\text{-}4S]^{2+}$ cluster is difficult to reduce with dithionite. Regardless of the behavior upon dithionite treatment, our analysis provides evidence that Pol δ isolated from yeast contains a $[4Fe\text{-}4S]^{2+}$ cluster, which upon purification partially (5–10%) breaks down to a $[3Fe\text{-}4S]^{1+}$ or $[3Fe\text{-}4S]^{0}$ cluster.

To verify the specificity and physiological relevance of Fe-S cluster binding to polymerases, we studied the effect of mutations in CysA or CysB on both Fe-S cluster binding and functionality of isolated Pol δ. The lethal double mutation C1059S C1074S in CysB of Pol3 disrupted its binding to both Pol31 and Pol32 upon isolation of Pol3 from cell extracts and in yeast two-hybrid experiments (**Fig. 4a** and **Supplementary Fig. 12**). The mutation further abrogated Fe-S cluster binding, as seen from chemical analysis and the loss of UV-vis and EPR signals (**Fig. 4b**,**c**). In marked contrast, lethal double mutation of CysA (C1012S C1027S) did not alter the subunit composition of the purified Pol δ complex and did not affect the Pol3 interactions in the two-hybrid analysis. Likewise, the Fe-S content, the UV-vis and EPR spectra were unchanged in comparison to the wild-type situation. These data further support the view that CysB binds a [4Fe-4S] cluster, whereas no evidence was obtained for Fe-S cluster binding to CysA. Hence, on the basis of the consensus zinc ribbon motif of CysA (C-X_2-C-X_{7-31}-C-X_2-C)[10] and the crystallographic data, CysA may bind zinc[14]. Neither set of mutations in the CTD of Pol3 affected its basal DNA polymerase activity (**Supplementary Fig. 13**), in agreement with Pol3 truncation mapping studies and structural comparisons with other B-family DNA polymerases that localize the catalytic domain N-terminal of the CTD[12].

CysA is an important determinant for PCNA binding

We then asked what the physiological function of the zinc-binding CysA motif may be. Processive DNA replication can be tested *in vitro* and depends on multiple protein and protein-DNA interactions, including those involving the processivity factor PCNA[32,33]. The latter protein is a circular homotrimeric clamp that coordinates DNA replication, recombination and repair processes and endows both stability and processivity to the replicating machinery. To address the role of the CysA motif in processive, lagging-strand DNA replication, we used isolated Pol δ preparations (Pol3, Pol31 and Pol32; **Supplementary Fig. 11**) for *in vitro* DNA synthesis in the presence of PCNA (**Supplementary Fig. 14**). Mutation of two cysteine residues of CysA (C1012S and C1027S) severely decreased PCNA-dependent replication processivity, documenting the importance of this metal center for polymerase function (**Fig. 5a**). An interaction between Pol δ and PCNA has previously been mapped to a C-terminal segment of the accessory subunit Pol32 and termed PIP (PCNA interaction protein) motif[33]. However, the Pol32-ΔPIP mutant form of Pol δ was almost fully proficient for processive DNA replication, underscoring its minor functional importance. The relative effects observed for the Pol3-CysA and Pol32-ΔPIP mutants shows the much higher importance of the CysA site compared to PIP for stability of the PCNA-polymerase complex on DNA. Hence, the CysA structural motif may represent the key binding site for PCNA on Pol δ,

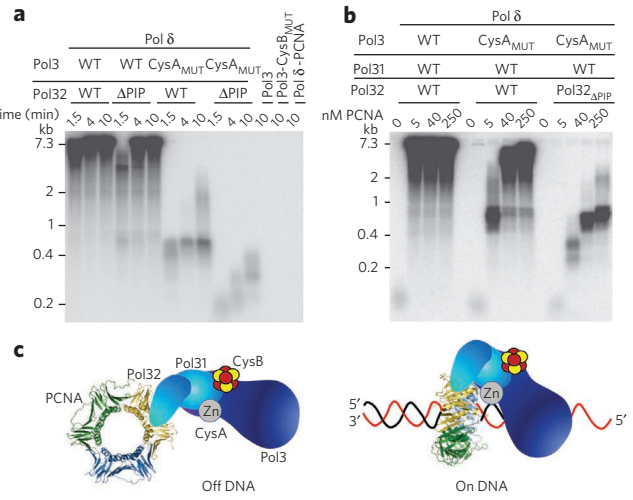

Figure 5 | The CysA motif of Pol δ is critical for processive DNA replication with PCNA. (**a**) Alkaline agarose gel electrophoresis of DNA replication products of assay with purified proteins as indicated. A phosphorimaging scan is shown. ΔPIP refers to truncated Pol32 (**Supplementary Fig. 11**). All complexes contain wild-type Pol31. The right-most lane is a control with wild-type Pol δ but without PCNA. Size markers are indicated on the left. (**b**) Assay as in **a** was carried out for 10 min with the indicated PCNA concentrations. (**c**) Model for the roles of the PIP and CysA motifs for PCNA interaction with Pol δ in solution (Off DNA) and in assembly with substrate (On DNA).

whereas the PIP motif may have an ancillary function. Consistent with this view, PCNA-dependent replication activity of Pol δ was almost completely abolished when both CysA and PIP binding sites were mutated (**Fig. 5a**). Used as controls for these experiments, the catalytic subunit Pol3 alone, the CysB mutant protein or a sample lacking PCNA showed no discernible processive DNA replication. To further substantiate the relative importance of the two PCNA binding sites of Pol δ, we varied the PCNA concentration in the *in vitro* replication assay containing either wild-type or CysA mutant Pol3 together with wild-type or ΔPIP-Pol32. Increasing PCNA concentrations relieved the replication defect of the CysA mutant, suggesting that under these conditions, interactions between PCNA and PIP partially rescue the replication defect (**Fig. 5b**). Indeed, when PIP was also absent, hardly any processive replication was observed. Taken together, these findings suggest a crucial role of CysA in PCNA–Pol δ complex formation, stability or both during on-DNA processive DNA replication (**Fig. 5c**). In contrast, the PIP binding site may be more relevant for off-DNA complex formation, such as recruitment of the enzyme to replication foci in the nucleus, as has been observed with other PIP box-containing proteins[33,34].

DISCUSSION

Our study identifies a previously unrecognized essential Fe-S cluster in the CTD of all yeast class B DNA polymerases, in addition to a Zn^{2+} ion bound on the other side of CTD[14]. Hence, this class of enzymes contains two different metal centers, which were shown to have distinct physiological roles. The presence of the Fe-S cluster was demonstrated by several *in vivo* and *in vitro* methods such as ^{55}Fe radiolabeling and purification of the DNA polymerase complex after induced expression of the enzyme in yeast, the native organism. Mutational and spectroscopic studies allowed us to define it as a [4Fe-4S] cluster that is coordinated by CysB, the second cysteine-rich motif in the CTD. The presence of an Fe-S cluster rather than Zn^{2+}, as originally suggested by a crystal structure of the CTD of Pol1, changes our understanding of DNA polymerase function and raises several questions regarding the precise physiological role of this Fe-S cluster. Our data clearly demonstrate that Pol3 becomes unstable in the absence of the Fe-S cluster (for example, upon Nfs1 depletion, as shown in western blots in **Supplementary Fig. 2**) and that the replication function is severely compromised owing to loss of accessory subunits essential for function at the replication fork (**Fig. 4**). This functional impairment caused by decreased complex stability may extend to the other DNA polymerases because the interaction between the various CTDs and their respective accessory proteins is a key determinant for the stability of the bound Fe-S cluster. It is likely that euryarchaeal D-family polymerases also bind an Fe-S cluster in the CysB motif. Interestingly, these polymerases contain a B subunit that has both phosphodiesterase-like and oligosaccharide-binding domains[6] and are thus predicted to share the principle of Fe-S cluster binding for accessory subunit recruitment with the eukaryotic polymerases. In the case of the translesion polymerase Pol ζ, the accessory protein Rev7 has a fold that is completely different from those of the B subunits of the other polymerases, and therefore a firm conclusion by analogy with Pol δ cannot be made and requires direct experimentation. However, the data do suggest that the Rev3-CTD may also be involved in Rev3-Rev7 interactions in addition to the interaction of the N-terminal region of the polymerase domain of Rev3 with Rev7 (ref. 35). Together, our findings assign essential roles to the Fe-S cluster: stabilization of the CTD to enable complex formation, maintenance of the catalytic polymerase subunit with its respective accessory proteins, or both. As an Fe-S cluster is intrinsically sensitive to oxidative stress, oxidative damage of the cluster may lead to gradual dissociation of the accessory subunits and decreased processivity at the replication fork. An attenuated rate of DNA replication during oxidative stress conditions may serve as a regulatory mechanism for polymerase activity.

In retrospect, the lability and complexity of Fe-S clusters may explain the previous difficulties in obtaining purified polymerase complex that is suitable for functional studies and crystallography. Purification of the catalytic subunit on its own invariably resulted in low yields and aggregation (detailed in Methods), possibly explaining why Pol3 could only be crystallized after truncation of the C terminus[12]. The Pol1-CTD in complex with Pol12 was crystallized with a Zn^{2+} ion in CysB after heterologous expression and purification from *E. coli*[14]. Our own purification experiments after expression in *E. coli* showed extreme lability of the Fe-S cluster of Pol1-CTD, necessitating anaerobic purification conditions to isolate the Fe-S cluster together with the protein. In general, misincorporation of non-native metal centers into metalloproteins is not unusual and has been encountered previously, especially upon overproduction or heterologous expression. For instance, replacement of Fe or an Fe-S cluster by Zn in *E. coli* has been reported

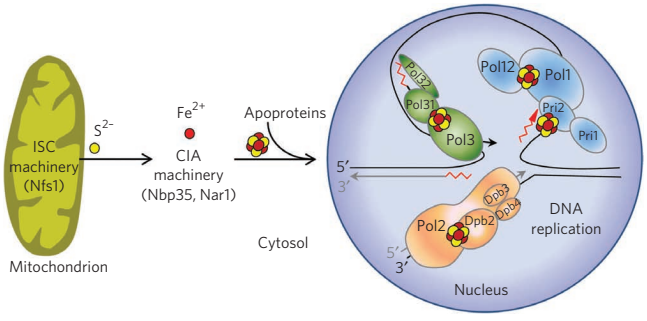

Figure 6 | Role of mitochondria and Fe-S cluster biogenesis in nuclear DNA replication. Assembly of Fe-S clusters on nuclear replicative DNA polymerases requires Fe-S protein biogenesis machineries located in the mitochondria (ISC machinery, iron-sulfur cluster assembly) and cytosol (CIA machinery, cytosolic iron-sulfur protein assembly), providing an explanation for the essential function of mitochondria for cell viability.

for *Clostridium pasteurianum* rubredoxin[36] or for the Fe-S cluster–containing scaffold protein IscU from *Haemophilus influenza*[37], respectively. Likewise, the CIA protein Nar1, containing two Fe-S clusters, does not contain its native metal centers after it is expressed in *E. coli*[38]. Zinc can be erroneously incorporated into the copper-binding protein azurin[39]. Ribonucleotide reductases of various bacteria, upon overexpression in *E. coli*, contain a dinuclear iron center, yet in their native state they have a dimanganese center[40,41]. Hence, these data imply that a number of proteins isolated as zinc-binding proteins may exist as Fe-S proteins inside the cell, emphasizing the importance of assessing the metal occupancy of a protein in its native organism.

Our data provide evidence for a previously unknown crucial function for the CysA zinc-binding segment in mediating DNA-dependent interactions between PCNA and the catalytic subunit of Pol δ (**Fig. 5c**). This protein interaction seems to operate alongside an earlier defined binding determinant, the C-terminal PIP motif of the accessory subunit Pol32. Because mutation of CysA was more detrimental to *in vitro* processive DNA replication than deletion of the PIP segment, CysA may be the major determinant for PCNA interaction with Pol δ on DNA. Notably, the function of the CysA motif may be more divergent than that of CysB, which seems to be conserved among all replicative DNA polymerases as a structural motif for the interaction with their respective essential accessory subunits. In Pol δ, Pol ε and Pol ζ, the CysA motif may serve a similar function, that is, mediating DNA-dependent interactions with PCNA, as all of these polymerases require PCNA for processive synthesis[42,43]. However, functional interactions between PCNA and Pol α have not been demonstrated[32,44], and therefore the functional role of the CysA motif in this enzyme awaits further investigation.

Our findings indicate that insertion of the Fe-S cluster into nuclear DNA polymerases depends on the function of not only the cytosolic but also the mitochondrial Fe-S protein biogenesis machineries (**Fig. 6**). The cysteine desulfurase Nfs1, if located only in the cytosol and nucleus, could not assist in the assembly of the Fe-S cluster into Pol3 (**Supplementary Fig. 3**). Thus, Nfs1, and presumably other members of the mitochondrial ISC assembly machinery[19], need to operate inside mitochondria to support Fe-S cluster insertion into polymerases. This finding shows, surprisingly, that mitochondria are essential for nuclear DNA replication, presumably because they act as sulfur donors for the DNA polymerase Fe-S cluster discovered here. This crucial task of mitochondria explains their indispensability for cell viability in virtually all eukaryotes and may be more basic than even respiration, which is dispensable in some organisms[19]. Interestingly, other steps of eukaryotic DNA and RNA metabolism involve Fe-S proteins including factors required for ribosome function in protein translation (Rli1), nucleotide excision repair and transcription (Rad3, named XPD in humans), DNA double strand break repair (FancJ) and chromosome segregation (Chl1)[19]. On one hand, the involvement of these proteins may explain the role of mitochondrial function in several DNA metabolism–related, neurodegenerative and cancer-linked phenotypes, including nuclear genome instability[45]. At least a subset of these disorders could originate from impaired Fe-S cluster assembly on these proteins and on the B-family DNA polymerases. On the other hand, the indispensable role of mitochondria in nuclear DNA and RNA metabolism suggests that eukaryotes, at some point in evolution, became dependent on these endosymbiontic organelles to express their genome.

METHODS

Yeast strains and plasmids. *Saccharomyces cerevisiae* W303-1A (*MAT**a**, ura3-1, ade2-1, trp1-1, his3-11,15* and *leu2-3,112*) was used as wild type and as a background strain for cells with genes under the control of galactose-regulatable promoters and/or encoding N- or C-terminally epitope-tagged proteins. Details of strains and plasmid constructs are in **Supplementary Methods** and **Supplementary Tables 1** and **2**.

Expression in *E. coli* and purification of CTDs. The pASK-IBA43plus plasmids (IBA) encoding the C-terminally Strep-tagged CTDs of Pol1, Pol2, Pol3 and Rev3 were transformed into BL21 *E. coli* cells. Induction with anhydrotetracycline hydrochloride (AHT, 4.3 μM) took place at $D_{600\,nm}$ of 0.5–0.7, at 30 °C for 16 h. Under these conditions, Pol1, Pol2 and Rev3 were totally insoluble. Inclusion bodies were solubilized in purification buffer (100 mM Tris-Cl, pH 8.0, 150 mM NaCl) containing 8 M urea. For Pol2, 6 M guanidinium hydrochloride was used instead of urea. To yield soluble CTDs, an overnight culture of *E. coli*, HMS174 (DE3) pLysS transformed with pASK-IBA43plus encoding the C-terminally Strep-tagged CTDs of Pol1, Pol2, Pol3 or Rev3 was diluted 100-fold into Terrific broth (24 g of yeast extract, 12 g of bactotryptone, 4 ml of glycerol, 12.5 g K_2HPO_4 and 2.31 g of KH_2PO_4 per liter) containing 3% (v/v) ethanol and was allowed to grow to a $D_{600\,nm}$ of 0.5 at 37 °C. The cultures were cooled down to 20 °C (~30 min), and benzyl alcohol (0.1 % v/v), betaine hydrochloride (1 mM), $FeCl_3$ (50 μM) and L-cysteine (100 μM) were added, followed by AHT. After ~16 h of expression at 20 °C, the cells were harvested and resuspended in anaerobic purification buffer. All subsequent steps were conducted in an anaerobic chamber (Coy), maintaining samples at 4 °C. The cell suspension was treated with 0.5 mg lysozyme per gram of cells for 30 min and was disrupted by sonication (three 30-s bursts, with 1-min cooling periods). After centrifugation at 100,000*g* for 45 min, the supernatant was mixed with one-tenth of its volume of high-capacity Strep-Tactin agarose (IBA) and homogenized for 1 h. The slurry was poured into a column and washed with 10 bed volumes of cold purification buffer, followed by elution with the same buffer containing 2 mM desthiobiotin. The proteins were analyzed by UV-vis spectroscopy and were frozen for EPR spectroscopy immediately after purification. For chemical analysis and SDS-PAGE, samples were shock-frozen and stored at −80 °C.

Purification of yeast Pol δ from yeast cells. Pol δ was purified from a yeast overproduction system[46]. *POL3* containing a cleavable N-terminal GST-purification tag, *POL31* and *POL32* were overexpressed from the galactose-inducible *GAL1-10* promoter in protease-deficient strain BJ2168 (*MAT**a**, ura3-52, trp1-289, leu2-3,112, prb1-1122, prc1-407, pep4-3*). After affinity purification on glutathione beads and removal of the GST tag by rhinoviral 3C protease, the preparation was further purified on a MonoS column. The SDS-PAGE shown in **Figure 4a** and **Supplementary Figure 11c** is of the MonoS eluates. Single and double cysteine-to-serine mutants were made using the QuikChange (Stratagene) protocol. Mutants were subjected to the same purification protocol. Because GST-tagged Pol3 was used for affinity purification, the presence of Pol31 and Pol32 in the Pol3-CysA mutant preparation and their absence from the Pol3-CysB mutant preparation indicates retention and defect in Pol3-Pol31 interactions in the mutants, respectively. After concentration to >2 mg ml^{-1} using Centricon filters, preparations of the wild-type and the CysA mutant, but not of the CysB mutant, showed an olive-yellow color. The Pol3 catalytic subunit on its own was prepared as described above, but after overexpression using only the pBL335 plasmid in BJ2168. The yield was invariably low, and the protein was aggregation prone. Contaminating three-subunit enzyme was removed by two consecutive MonoS column steps (the single Pol3 subunit elutes before Pol δ). Pol δ preparations with Pol32-ΔPIP containing either the wild-type or CysA form of Pol3 were overproduced in strain PY117 (*MAT**a**, ura3-52, trp1-289, leu2-3,112, his3-11,15, prb1-1122, pep4-3, pol32-Δ::HIS3*), a *pol32Δ* derivative of BJ2168 (ref. 33). Complex purification was performed in the same way as for wild-type.

Single-strand DNA replication assays. PCNA, RFC and RPA were purified as described[47–49]. Assays (60 μl) contained 20 mM Tris-HCl pH 7.8, 1 mM DTT, 100 μg ml^{-1} bovine serum albumin, 8 mM magnesium acetate, 0.5 mM ATP, 100 μM each of dCTP, dGTP and dTTP, 10 μM of [α-^{32}P]dATP, 100 mM NaCl, 2 nM of singly primed (36 base pairs, complementary to nucleotides 6330–6295) single-stranded M13mp18 DNA, 500 nM of RPA and 5 nM of PCNA (or PCNA concentration indicated in **Fig. 5**). PCNA was loaded onto the primed DNA by incubation with 5 nM RFC at 30 °C for 1 min, and replication was started by adding (mutant) Pol δ or Pol3. Aliquots (18 μl) were taken at various time points, and replication was stopped by the addition of 2 μl 100 mM EDTA and 3% SDS. After incubating at 50 °C for 10 min, 45 μl of precipitation solution (2.5 M ammonium acetate, 20 μg ml^{-1} sonicated salmon sperm DNA, 1 mM EDTA and 0.05 mg ml^{-1} linear acrylamide (Ambion Technologies)) was added, followed by ethanol precipitation. The dissolved pellet was analyzed by electrophoresis on a 1% alkaline agarose gel. Gels were dried and documented by PhosphorImager analysis (GE Healthcare).

EPR and UV-vis spectroscopy. EPR spectra were recorded with a Bruker EMX-6/1 X-band spectrometer containing an ER-041 XG microwave bridge, ER-041-1161 frequency counter, EMX-1101 power supply, ER-070 magnet, EMX-032T Hall field probe, ER-4102 Universal TE102 rectangular cavity and Oxford Instruments helium flow cryostat ESR-900. Data acquisition and manipulation were performed with the Bruker WINEPR software. For spin quantification, 1 mM $CuSO_4$ in 2 M $NaClO_4$ and 10 mM HCl was used. UV-vis spectra were recorded on a Jasco V-550 spectrophotometer. For EPR and UV-vis spectroscopy, the proteins were in anaerobic purification buffer and treated with sodium dithionite (2 mM) or potassium

ferricyanide (2 mM) when applicable. Samples were transferred inside the anaerobic chamber to stoppered anaerobic quartz cuvettes (Hellma) or Ilmasil-PN high-purity quartz EPR tubes. EPR samples were capped with rubber seals and shock-frozen outside the anaerobic chamber in liquid nitrogen.

Additional methods. ^{55}Fe incorporation, cloning, yeast two-hybrid analysis, cysteine mutagenesis, and chemical analysis of iron and acid-labile sulfide are described in the **Supplementary Methods**.

Received 19 July 2011; accepted 3 October 2011; published online 27 November 2011

References

1. Johansson, E. & Macneill, S.A. The eukaryotic replicative DNA polymerases take shape. *Trends Biochem. Sci.* **35**, 339–347 (2010).
2. Nick McElhinny, S.A., Gordenin, D.A., Stith, C.M., Burgers, P.M. & Kunkel, T.A. Division of labor at the eukaryotic replication fork. *Mol. Cell* **30**, 137–144 (2008).
3. Pursell, Z.F., Isoz, I., Lundström, E.B., Johansson, E. & Kunkel, T.A. Yeast DNA polymerase ε participates in leading-strand DNA replication. *Science* **317**, 127–130 (2007).
4. Burgers, P.M. *et al.* Eukaryotic DNA polymerases: proposal for a revised nomenclature. *J. Biol. Chem.* **276**, 43487–43490 (2001).
5. Mäkiniemi, M. *et al.* A novel family of DNA-polymerase-associated B subunits. *Trends Biochem. Sci.* **24**, 14–16 (1999).
6. Baranovskiy, A.G. *et al.* X-ray structure of the complex of regulatory subunits of human DNA polymerase δ. *Cell Cycle* **7**, 3026–3036 (2008).
7. Nelson, J.R., Lawrence, C.W. & Hinkle, D.C. Thymine-thymine dimer bypass by yeast DNA polymerase ζ. *Science* **272**, 1646–1649 (1996).
8. Prakash, S., Johnson, R.E. & Prakash, L. Eukaryotic translesion synthesis DNA polymerases: specificity of structure and function. *Annu. Rev. Biochem.* **74**, 317–353 (2005).
9. Bemark, M., Khamlichi, A.A., Davies, S.L. & Neuberger, M.S. Disruption of mouse polymerase ζ (Rev3) leads to embryonic lethality and impairs blastocyst development *in vitro*. *Curr. Biol.* **10**, 1213–1216 (2000).
10. Krishna, S.S., Majumdar, I. & Grishin, N.V. Structural classification of zinc fingers: survey and summary. *Nucleic Acids Res.* **31**, 532–550 (2003).
11. Tahirov, T.H., Makarova, K.S., Rogozin, I.B., Pavlov, Y.I. & Koonin, E.V. Evolution of DNA polymerases: an inactivated polymerase-exonuclease module in Pol ε and a chimeric origin of eukaryotic polymerases from two classes of archaeal ancestors. *Biol. Direct* **4**, 11 (2009).
12. Swan, M.K., Johnson, R.E., Prakash, L., Prakash, S. & Aggarwal, A.K. Structural basis of high-fidelity DNA synthesis by yeast DNA polymerase δ. *Nat. Struct. Mol. Biol.* **16**, 979–986 (2009).
13. Evanics, F., Maurmann, L., Yang, W.W. & Bose, R.N. Nuclear magnetic resonance structures of the zinc finger domain of human DNA polymerase-α. *Biochim. Biophys. Acta* **1651**, 163–171 (2003).
14. Klinge, S., Núñez-Ramírez, R., Llorca, O. & Pellegrini, L. 3D architecture of DNA Pol α reveals the functional core of multi-subunit replicative polymerases. *EMBO J.* **28**, 1978–1987 (2009).
15. Mizuno, T., Yamagishi, K., Miyazawa, H. & Hanaoka, F. Molecular architecture of the mouse DNA polymerase α-primase complex. *Mol. Cell. Biol.* **19**, 7886–7896 (1999).
16. Dua, R., Levy, D.L. & Campbell, J.L. Analysis of the essential functions of the C-terminal protein/protein interaction domain of *Saccharomyces cerevisiae* pol ε and its unexpected ability to support growth in the absence of the DNA polymerase domain. *J. Biol. Chem.* **274**, 22283–22288 (1999).
17. Sanchez Garcia, J., Ciufo, L.F., Yang, X., Kearsey, S.E. & MacNeill, S.A. The C-terminal zinc finger of the catalytic subunit of DNA polymerase δ is responsible for direct interaction with the B-subunit. *Nucleic Acids Res.* **32**, 3005–3016 (2004).
18. Chanet, R. & Heude, M. Characterization of mutations that are synthetic lethal with *pol3–13*, a mutated allele of DNA polymerase delta in *Saccharomyces cerevisiae*. *Curr. Genet.* **43**, 337–350 (2003).
19. Lill, R. Function and biogenesis iron-sulphur proteins. *Nature* **460**, 831–838 (2009).
20. Hausmann, A. *et al.* The eukaryotic P-loop NTPase Nbp35: an essential component of the cytosolic and nuclear iron-sulfur protein assembly machinery. *Proc. Natl. Acad. Sci. USA* **102**, 3266–3271 (2005).
21. Zhang, Y. *et al.* Dre2, a conserved eukaryotic Fe/S cluster protein, functions in cytosolic Fe/S protein biogenesis. *Mol. Cell. Biol.* **28**, 5569–5582 (2008).
22. Netz, D.J.A. *et al.* Tah18 transfers electrons to Dre2 in cytosolic iron-sulfur protein biogenesis. *Nat. Chem. Biol.* **6**, 758–765 (2010).
23. Roy, A., Solodovnikova, N., Nicholson, T., Antholine, W. & Walden, W.E. A novel eukaryotic factor for cytosolic Fe-S cluster assembly. *EMBO J.* **22**, 4826–4835 (2003).
24. Netz, D.J.A., Pierik, A.J., Stümpfig, M., Mühlenhoff, U. & Lill, R. The Cfd1-Nbp35 complex acts as a scaffold for iron-sulfur protein assembly in the yeast cytosol. *Nat. Chem. Biol.* **3**, 278–286 (2007).
25. Balk, J., Pierik, A.J., Netz, D.J.A., Mühlenhoff, U. & Lill, R. The hydrogenase-like Nar1p is essential for maturation of cytosolic and nuclear iron-sulphur proteins. *EMBO J.* **23**, 2105–2115 (2004).
26. Balk, J., Netz, D.J.A., Tepper, K., Pierik, A.J. & Lill, R. The essential WD40 protein Cia1 is involved in a late step of cytosolic and nuclear iron-sulfur protein assembly. *Mol. Cell. Biol.* **25**, 10833–10841 (2005).
27. Kispal, G., Csere, P., Prohl, C. & Lill, R. The mitochondrial proteins Atm1p and Nfs1p are required for biogenesis of cytosolic Fe/S proteins. *EMBO J.* **18**, 3981–3989 (1999).
28. Klinge, S., Hirst, J., Maman, J.D., Krude, T. & Pellegrini, L. An iron-sulfur domain of the eukaryotic primase is essential for RNA primer synthesis. *Nat. Struct. Mol. Biol.* **14**, 875–877 (2007).
29. Burgers, P.M. & Gerik, K.J. Structure and processivity of two forms of *Saccharomyces cerevisiae* DNA polymerase δ. *J. Biol. Chem.* **273**, 19756–19762 (1998).
30. Orme-Johnson, W.H. & Orme-Johnson, A.R. Iron-sulfur proteins: the problem of determining cluster type. in *Iron-Sulfur Proteins* (ed. Spiro, T.G.) 67–95 (Wiley, 1982).
31. Kent, T.A. *et al.* Mössbauer studies of beef heart aconitase: evidence for facile interconversions of iron-sulfur clusters. *Proc. Natl. Acad. Sci. USA* **79**, 1096–1100 (1982).
32. Tsurimoto, T. & Stillman, B. Multiple replication factors augment DNA synthesis by the two eukaryotic DNA polymerases, α and δ. *EMBO J.* **8**, 3883–3889 (1989).
33. Johansson, E., Garg, P. & Burgers, P.M. The Pol32 subunit of DNA polymerase δ contains separable domains for processive replication and proliferating cell nuclear antigen (PCNA) binding. *J. Biol. Chem.* **279**, 1907–1915 (2004).
34. Montecucco, A. *et al.* DNA ligase I is recruited to sites of DNA replication by an interaction with proliferating cell nuclear antigen: identification of a common targeting mechanism for the assembly of replication factories. *EMBO J.* **17**, 3786–3795 (1998).
35. Hara, K. *et al.* Crystal structure of human REV7 in complex with a human REV3 fragment and structural implication of the interaction between DNA polymerase ζ and REV1. *J. Biol. Chem.* **285**, 12299–12307 (2010).
36. Dauter, Z., Wilson, K.S., Sieker, L.C., Moulis, J.M. & Meyer, J. Zinc- and iron-rubredoxins from *Clostridium pasteurianum* at atomic resolution: a high-precision model of a ZnS_4 coordination unit in a protein. *Proc. Natl. Acad. Sci. USA* **93**, 8836–8840 (1996).
37. Ramelot, T.A. *et al.* Solution NMR structure of the iron-sulfur cluster assembly protein U (IscU) with zinc bound at the active site. *J. Mol. Biol.* **344**, 567–583 (2004).
38. Urzica, E., Pierik, A.J., Mühlenhoff, U. & Lill, R. Crucial role of conserved cysteine residues in the assembly of two iron-sulfur clusters on the CIA protein Nar1. *Biochemistry* **48**, 4946–4958 (2009).
39. Nar, H. *et al.* Characterization and crystal structure of zinc azurin, a by-product of heterologous expression in *Escherichia coli* of *Pseudomonas aeruginosa* copper azurin. *Eur. J. Biochem.* **205**, 1123–1129 (1992).
40. Abbouni, B., Oehlmann, W., Stolle, P., Pierik, A.J. & Auling, G. Electron paramagnetic resonance (EPR) spectroscopy of the stable-free radical in the native metallo-cofactor of the manganese-ribonucleotide reductase (Mn-RNR) of *Corynebacterium glutamicum*. *Free Radic. Res.* **43**, 943–950 (2009).
41. Boal, A.K., Cotruvo, J.A. Jr., Stubbe, J. & Rosenzweig, A.C. Structural basis for activation of class Ib ribonucleotide reductase. *Science* **329**, 1526–1530 (2010).
42. Burgers, P.M.J. *Saccharomyces cerevisiae* replication factor C. II. Formation and activity of complexes with the proliferating cell nuclear antigen and with DNA polymerases δ and ε. *J. Biol. Chem.* **266**, 22698–22706 (1991).
43. Garg, P., Stith, C.M., Majka, J. & Burgers, P.M.J. Proliferating cell nuclear antigen promotes translesion synthesis by DNA polymerase ζ. *J. Biol. Chem.* **280**, 23446–23450 (2005).
44. Wong, S.W. *et al.* DNA polymerases α and δ are immunologically and structurally distinct. *J. Biol. Chem.* **264**, 5924–5928 (1989).
45. Veatch, J.R., McMurray, M.A., Nelson, Z.W. & Gottschling, D.E. Mitochondrial dysfunction leads to nuclear genome instability via an iron-sulfur cluster defect. *Cell* **137**, 1247–1258 (2009).
46. Fortune, J.M., Stith, C.M., Kissling, G.E., Burgers, P.M. & Kunkel, T.A. RPA and PCNA suppress formation of large deletion errors by yeast DNA polymerase δ. *Nucleic Acids Res.* **34**, 4335–4341 (2006).
47. Ayyagari, R., Impellizzeri, K.J., Yoder, B.L., Gary, S.L. & Burgers, P.M. A mutational analysis of the yeast proliferating cell nuclear antigen indicates distinct roles in DNA replication and DNA repair. *Mol. Cell. Biol.* **15**, 4420–4429 (1995).
48. Gomes, X.V., Gary, S.L. & Burgers, P.M. Overproduction in *Escherichia coli* and characterization of yeast replication factor C lacking the ligase homology domain. *J. Biol. Chem.* **275**, 14541–14549 (2000).
49. Henricksen, L.A., Umbricht, C.B. & Wold, M.S. Recombinant replication protein A: expression, complex formation, and functional characterization. *J. Biol. Chem.* **269**, 11121–11132 (1994).

Acknowledgments

We thank B. Yoder for yeast two-hybrid analysis and M. Reuter for help with cloning. This work was supported by grant GM032431 from the US National Institutes of Health (P.M.J.B.), the Deutsche Forschungsgemeinschaft (SFB 593, Gottfried-Wilhelm Leibniz program, and GRK 1216), Rhön Klinikum, von Behring-Röntgen Stiftung, LOEWE-Program of State Hessen, Max-Planck Gesellschaft and Fonds der Chemischen Industrie.

Author contributions

All authors performed experiments. D.J.A.N., R.L., P.M.J.B. and A.J.P. designed experiments, analyzed data and wrote the manuscript.

Competing financial interests

The authors declare no competing financial interests.

Additional information

Supplementary information is available online at http://www.nature.com/naturechemicalbiology/. Reprints and permissions information is available online at http://www.nature.com/reprints/index.html. Correspondence and requests for materials should be addressed to R.L. (lill@staff.uni-marburg.de), P.M.J.B. (burgers@biochem.wustl.edu) or A.J.P. (pierik@staff.uni-marburg.de).

SUPPLEMENTARY INFORMATION

Eukaryotic DNA polymerases require an iron-sulfur cluster for the formation of active complexes

Daili J. A. Netz[1], Carrie M. Stith[2], Martin Stümpfig[1], Gabriele Köpf[1], Daniel Vogel[1], Heide M. Genau[1], Joseph L. Stodola[2], Roland Lill[1*], Peter M. J. Burgers[2*] & Antonio J. Pierik[1*]

[1]Institut für Zytobiologie und Zytopathologie, Philipps-Universität Marburg, Robert-Koch-Strasse 6, D-35033 Marburg, Germany.
[2]Department of Biochemistry and Molecular Biophysics, Washington University School of Medicine, St. Louis, Missouri 63110, USA.

* To whom correspondence should be addressed. E-mail: lill@staff.uni-marburg.de, burgers@biochem.wustl.edu, pierik@staff.uni-marburg.de

Supplementary Figures 1-14

Supplementary Tables 1-2

Supplementary Methods and References

Nature Chemical Biology: doi:10.1038/nchembio.721

Supplementary Results

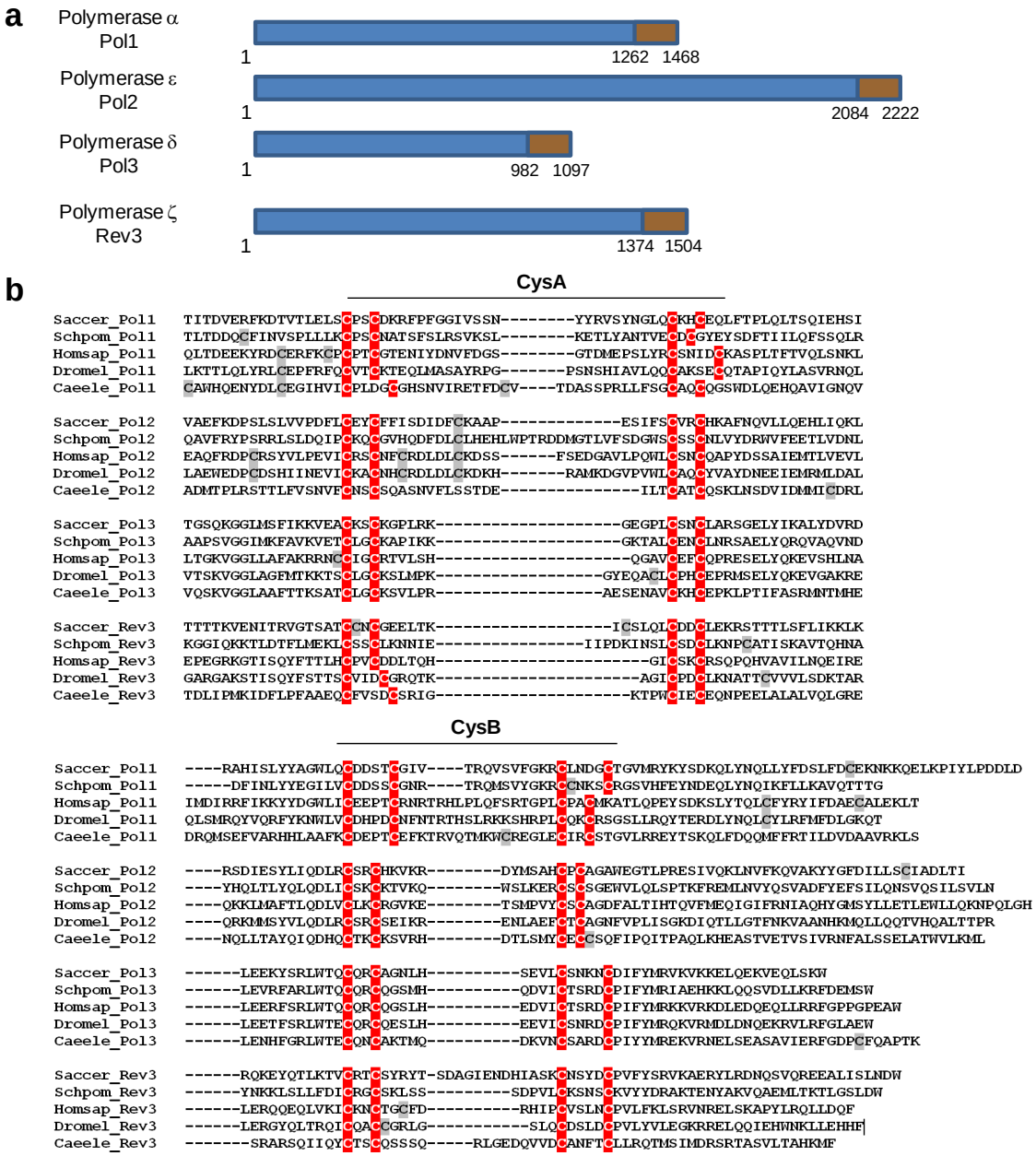

Supplementary Figure 1. Eukaryotic B-family DNA polymerases contain eight conserved cysteine residues in their C-terminal domain (CTD). a, Schematic representation of the *Saccharomyces cerevisiae* B-family DNA polymerases with amino acid positions demarking the CTDs (in brown). **b**, Amino acid sequence alignment of the CTDs shows two motifs of four cysteine residues, CysA and CysB which are involved in metal binding. Abbreviations: Saccer, *S. cerevisiae*; Schpom, *Schizosaccharomyces pombe*; Homsap, *Homo sapiens*; Dromel, *Drosophila melanogaster*; Caeele, *Caenorhabditis elegans*. Cysteine residues which are considered to coordinate metal ions have been highlighted in red, other cysteine residues in grey.

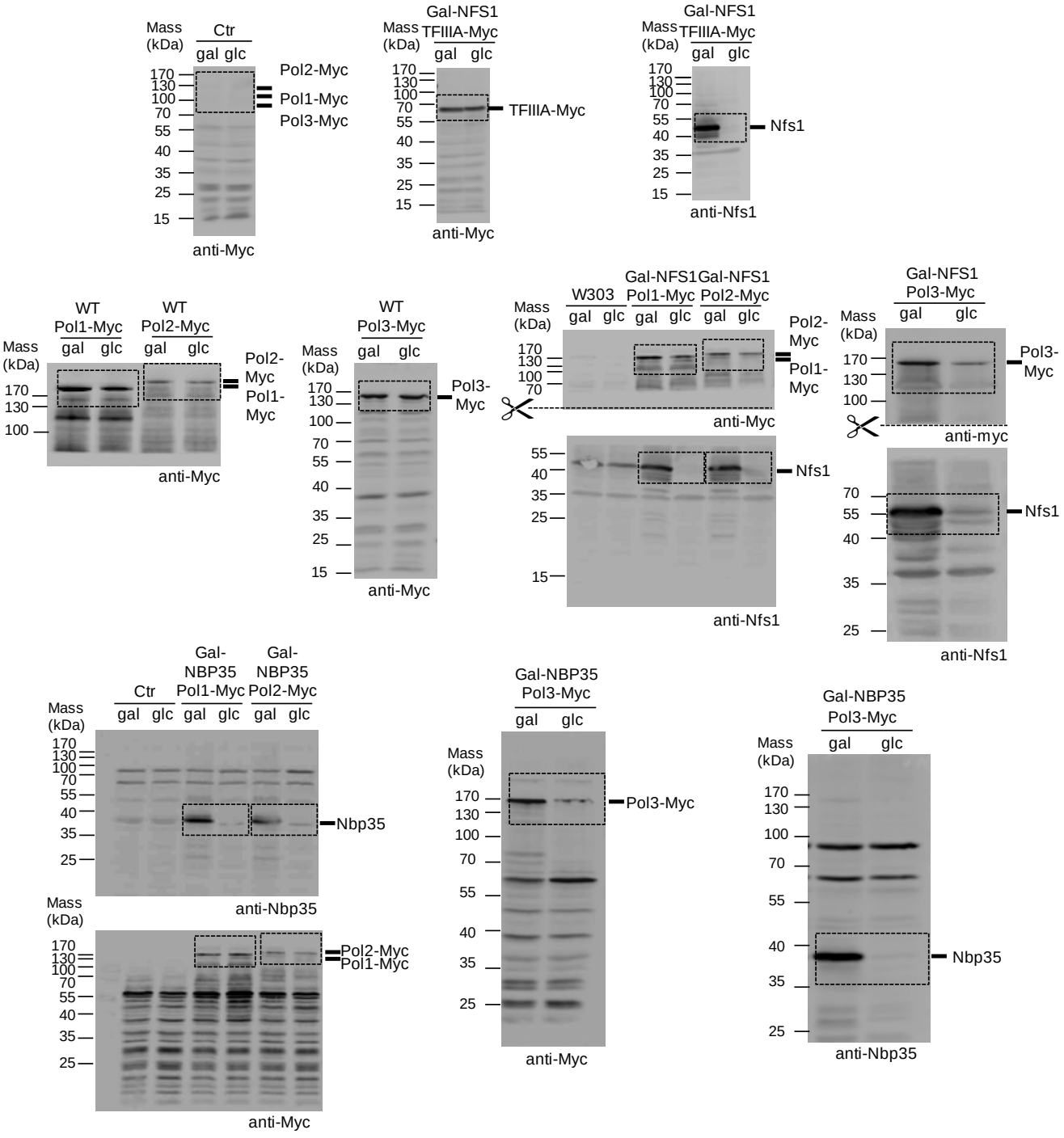

Supplementary Figure 2. Immunoblots for the indicated (tagged) proteins in the cell extracts subjected to ^{55}Fe incorporation in Figure 1a. Proteins were visualized by immunostaining using specific antibodies and chemiluminescence detection by a CCD camera. Hatched boxes denote areas of particular interest (target of immunoprecipitation or protein depleted). The positions of molecular mass markers are indicated.

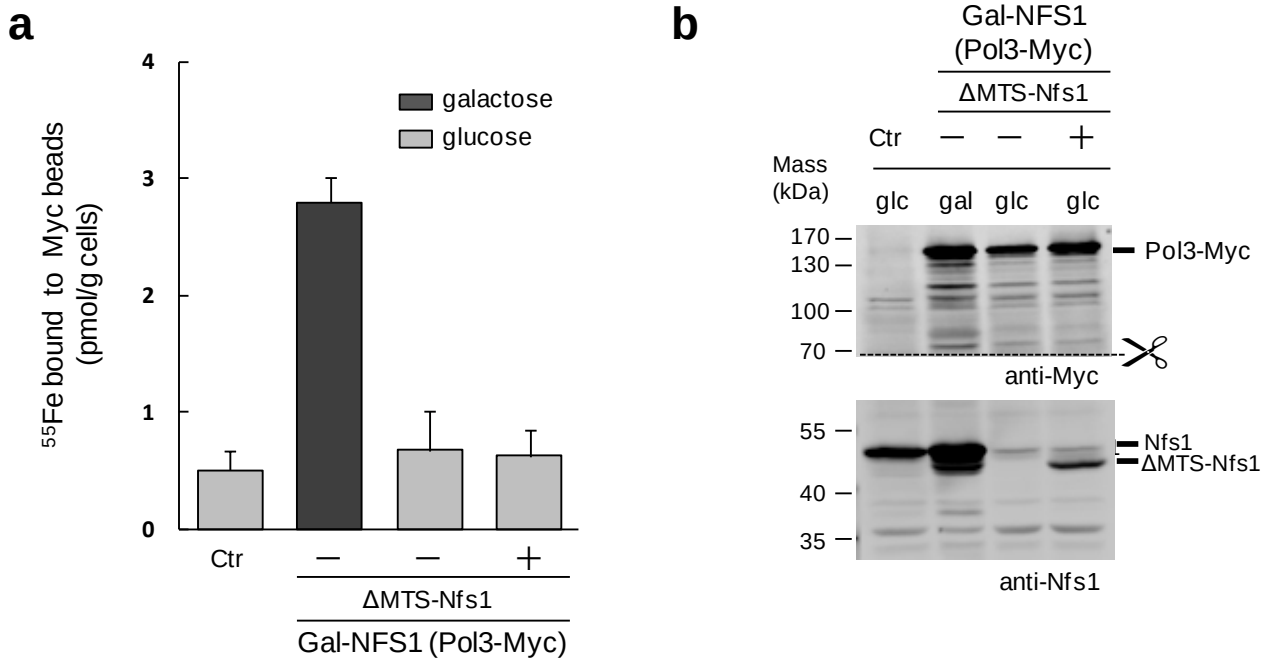

Supplementary Figure 3. A cytosolic version of cysteine desulfurase Nfs1 does not support Fe-S cluster assembly on Pol3-Myc. Gal-NFS1 cells with the *NFS1* gene under the control of the *GAL1-10* (Gal) promoter were transformed with a plasmid (+) encoding a cytosolic form[1] of Nfs1 (lacking amino acid residues 1-94, ΔMTS-Nfs1) or with an empty plasmid (-). **a,** ^{55}Fe radiolabelling and immunoprecipitation was performed as in Fig. 1 using wild-type cells (Ctr) or the indicated Gal-NFS1 cells carrying genomically Myc-tagged Pol3. The data for wild-type cells and the galactose bar correspond to Fig. 1a in the main text. **b,** Cell extracts from **a** were analyzed by immunoblotting to show the presence of Pol3-Myc, the depletion of mitochondrial Nfs1, and the synthesis of the slightly shorter ΔMTS-Nfs1 protein. Error bars, s.d. ($n \geq 3$).

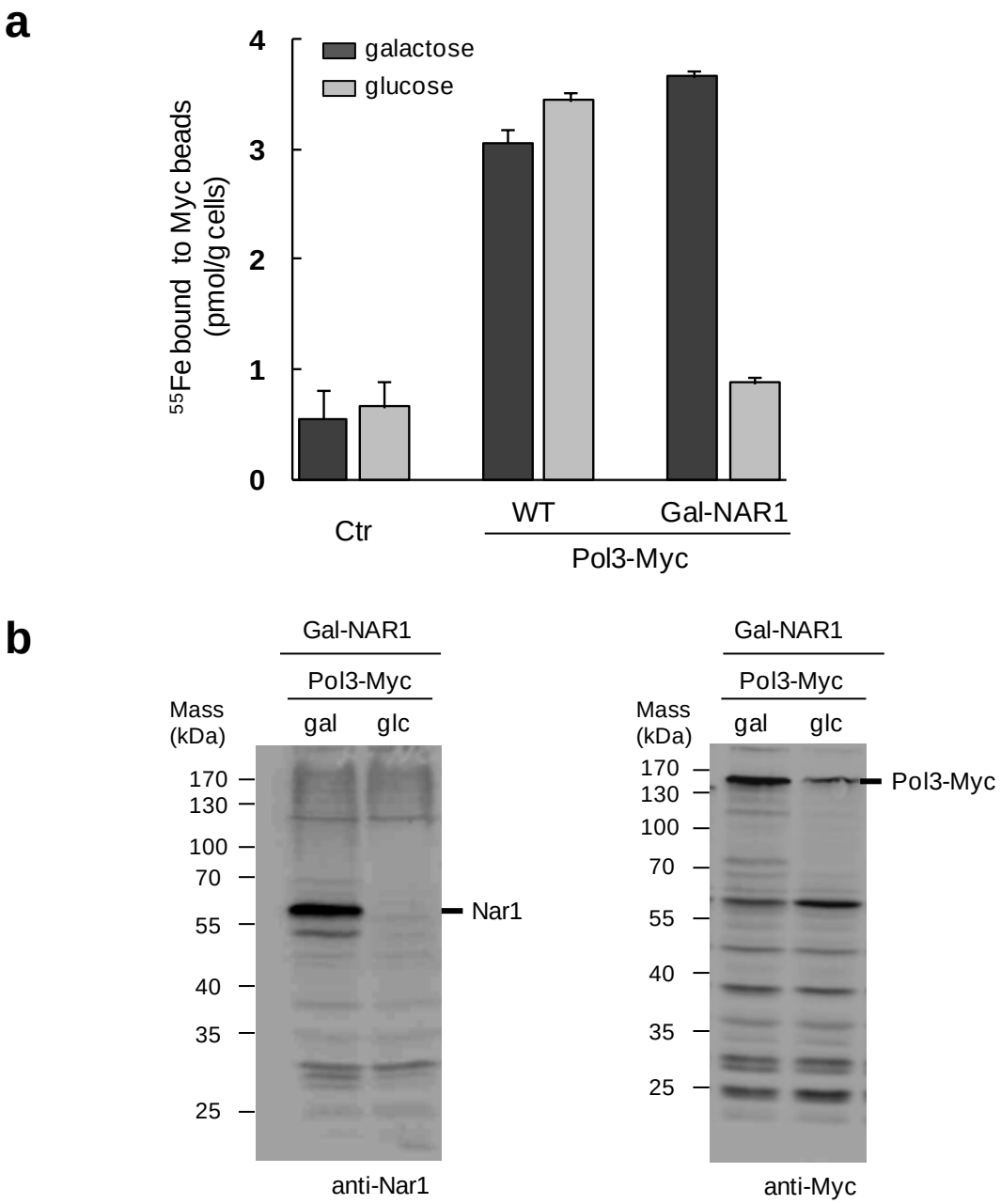

Supplementary Figure 4. Depletion of the cytosolic CIA protein Nar1 leads to loss of radioactive iron associated with Pol3-Myc. a, ^{55}Fe radiolabelling and immunoprecipitation was performed as in Fig. 1 using wild-type cell extracts (Ctr), or extracts from wild-type (WT) and Gal-NAR1 cells carrying genomically Myc-tagged Pol3. Gal-NAR1 cells express the *NAR1* gene under the control of the *GAL1-10* (Gal) promoter. The data for Ctr and WT correspond to Fig. 1a in the main text. **b,** Immunoblots of cell extracts from **a**. The indicated (tagged) proteins were visualized by immunostaining using specific antibodies and chemiluminescence detection by a CCD camera. The positions of molecular mass markers are indicated. Error bars, s.d. ($n \geq 3$).

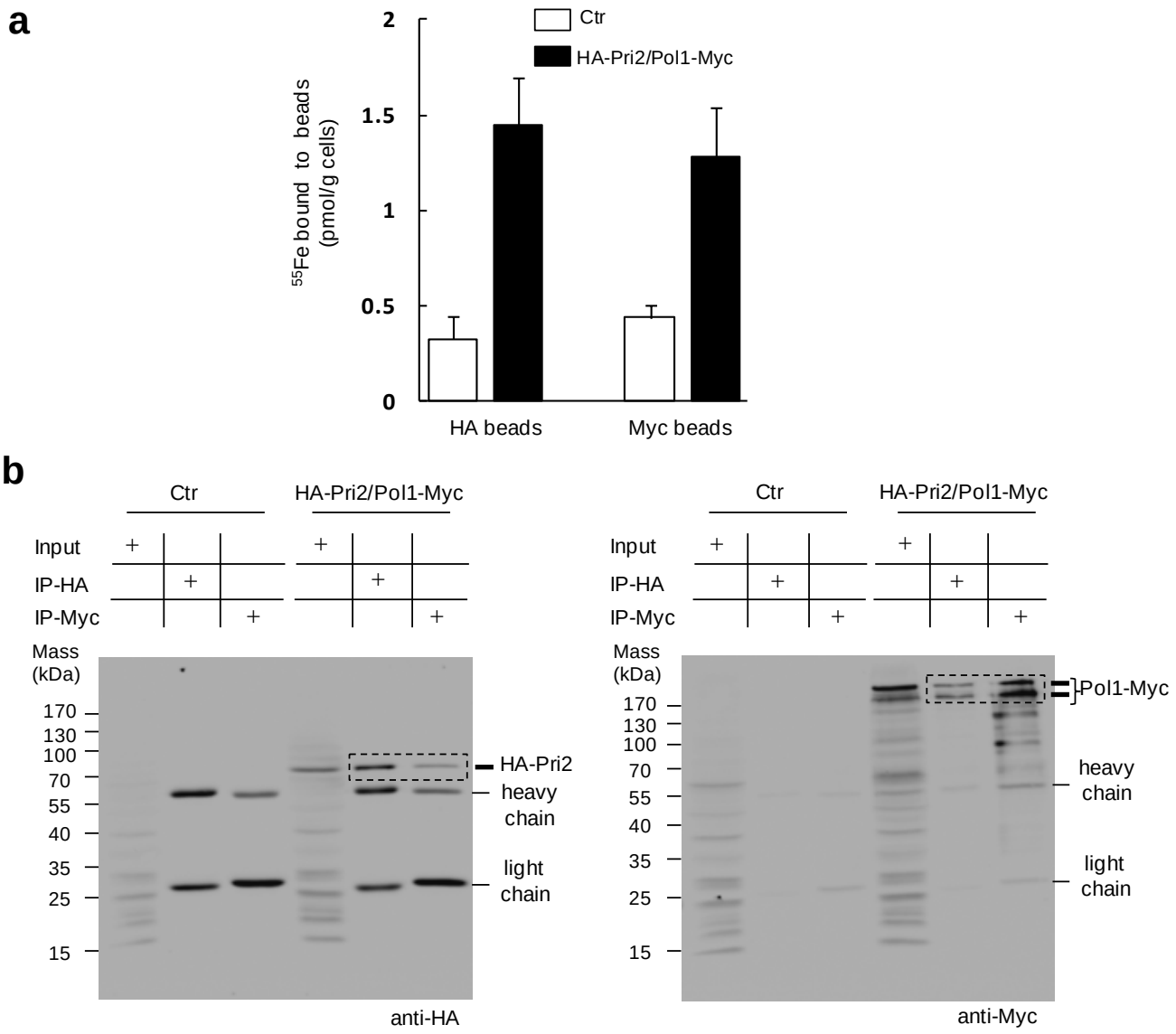

Supplementary Figure 5. Comparison of ^{55}Fe associated with endogenous levels of Pol1 and the [4Fe-4S] cluster-containing primase subunit Pri2. a, ^{55}Fe radiolabelling and immunoprecipitation was performed as in Fig. 1 using wild-type cells (Ctr) or a yeast strain with genomically integrated Pol1-Myc/HA-Pri2. Cells were grown in iron-free SC medium supplemented with galactose. **b,** Co-immunoprecipitation of HA-Pri2 and Pol1-Myc with anti-HA or anti-Myc beads. The strains described in **a** were grown on regular SC medium supplemented with galactose and lysates were prepared with glass beads (Input). After centrifugation, the obtained supernatants were separated into two aliquots and incubated with anti-HA or anti-Myc agarose beads. The beads were washed (IP-HA and IP-Myc) and analyzed by SDS-PAGE and immunoblotting using the indicated monoclonal antibodies. Bands labeled heavy and light chain are cross-reactive IgG subunits released from beads. The intensity of the HA-Pri2 band in the Myc beads was 20% of the same band in the HA beads (boxed bands in left blot) as quantified from the chemiluminescence recording of the CCD camera. Error bars, s.d. ($n \geq 3$).

Nature Chemical Biology: doi:10.1038/nchembio.721

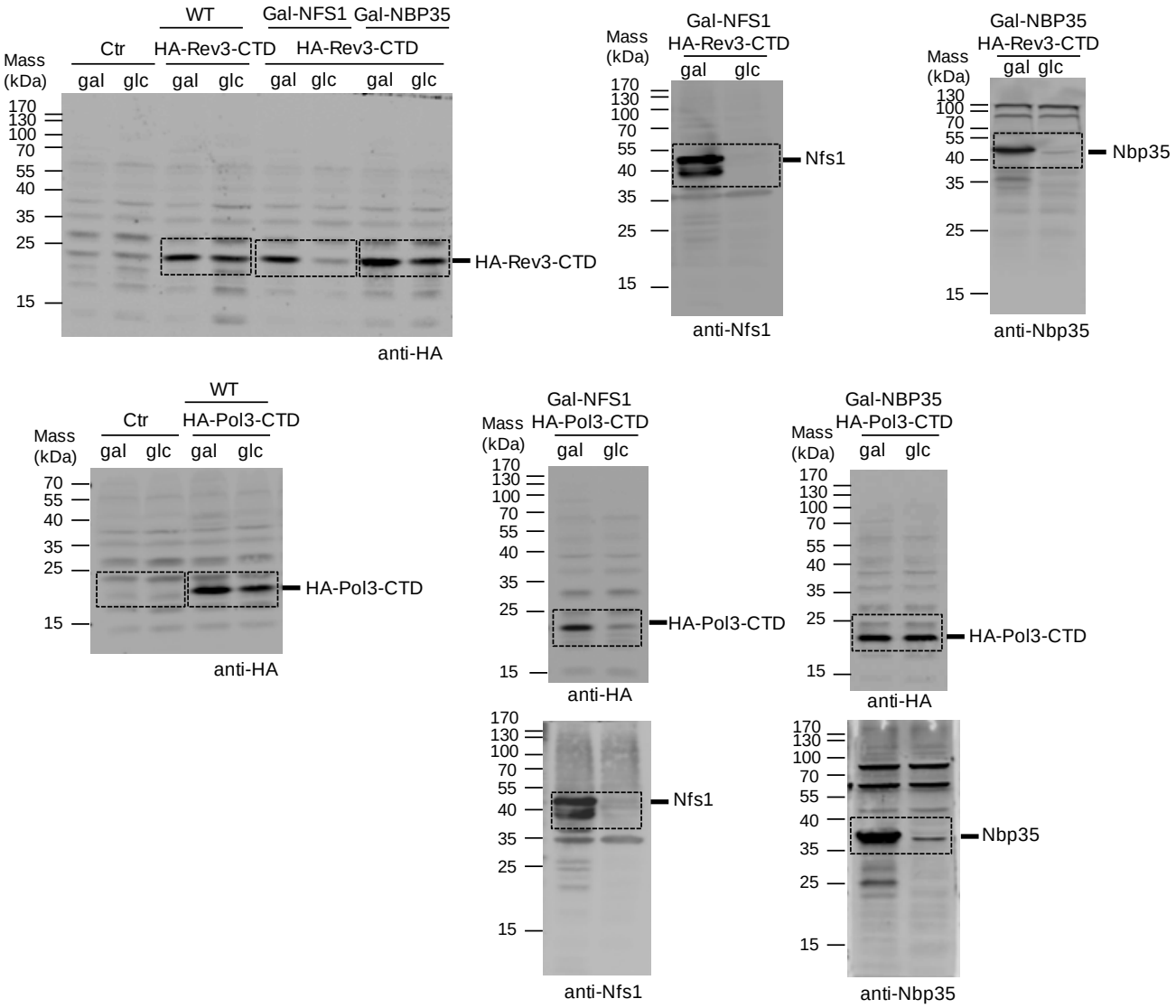

Supplementary Figure 6. Immunoblots for the indicated (tagged) proteins in the cell extracts subjected to ^{55}Fe incorporation in Figure 1b. Proteins were visualized by immunostaining using specific antibodies and chemiluminescence detection by a CCD camera. Hatched boxes denote areas of particular interest (target of immunoprecipitation or protein depleted). The positions of molecular mass markers are indicated.

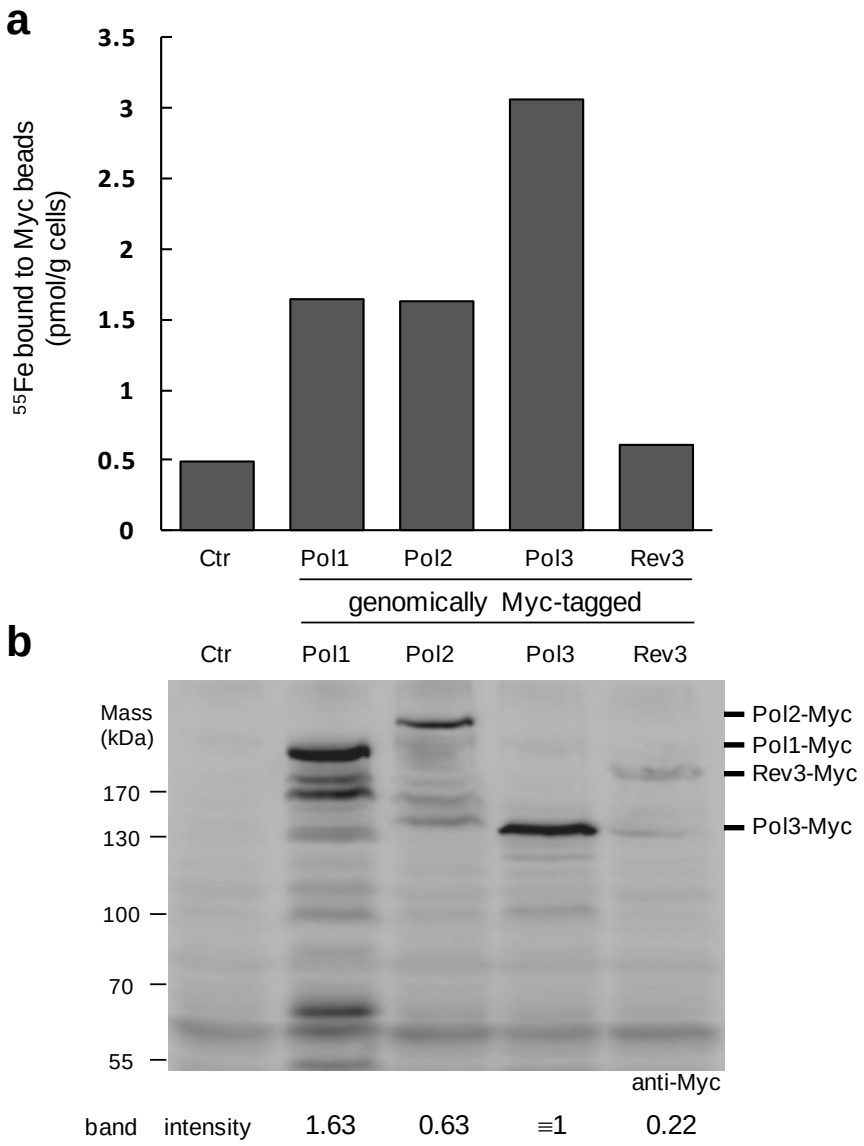

Supplementary Figure 7. Comparison of the expression levels of yeast B-family DNA polymerases shows that Rev3 has a low abundance. a, Wild-type yeast cells (Ctr) and cells carrying genomically Myc-tagged polymerases were grown in Fe-free galactose-containing SC medium. Cell extracts were prepared and an immunoprecipitation of the Myc-tagged, indicated polymerases was performed. Co-immunoprecipitated ^{55}Fe was analyzed by scintillation counting. Data for Ctr, Pol1, Pol2 and Pol3 correspond to the Ctr and the WT bars of Fig. 1a in the main text. **b,** The indicated (tagged) proteins in cell extracts from **a** were visualized by immunostaining using specific antibodies and chemiluminescence detection by a CCD camera. The summed intensities (bottom) of discrete bands with molecular mass above 120 kDa were normalized to the intensity of a cross-reactive band at ~60 kDa. The positions of molecular mass markers are indicated. Error bars, s.d. ($n \geq 3$).

Nature Chemical Biology: doi:10.1038/nchembio.721

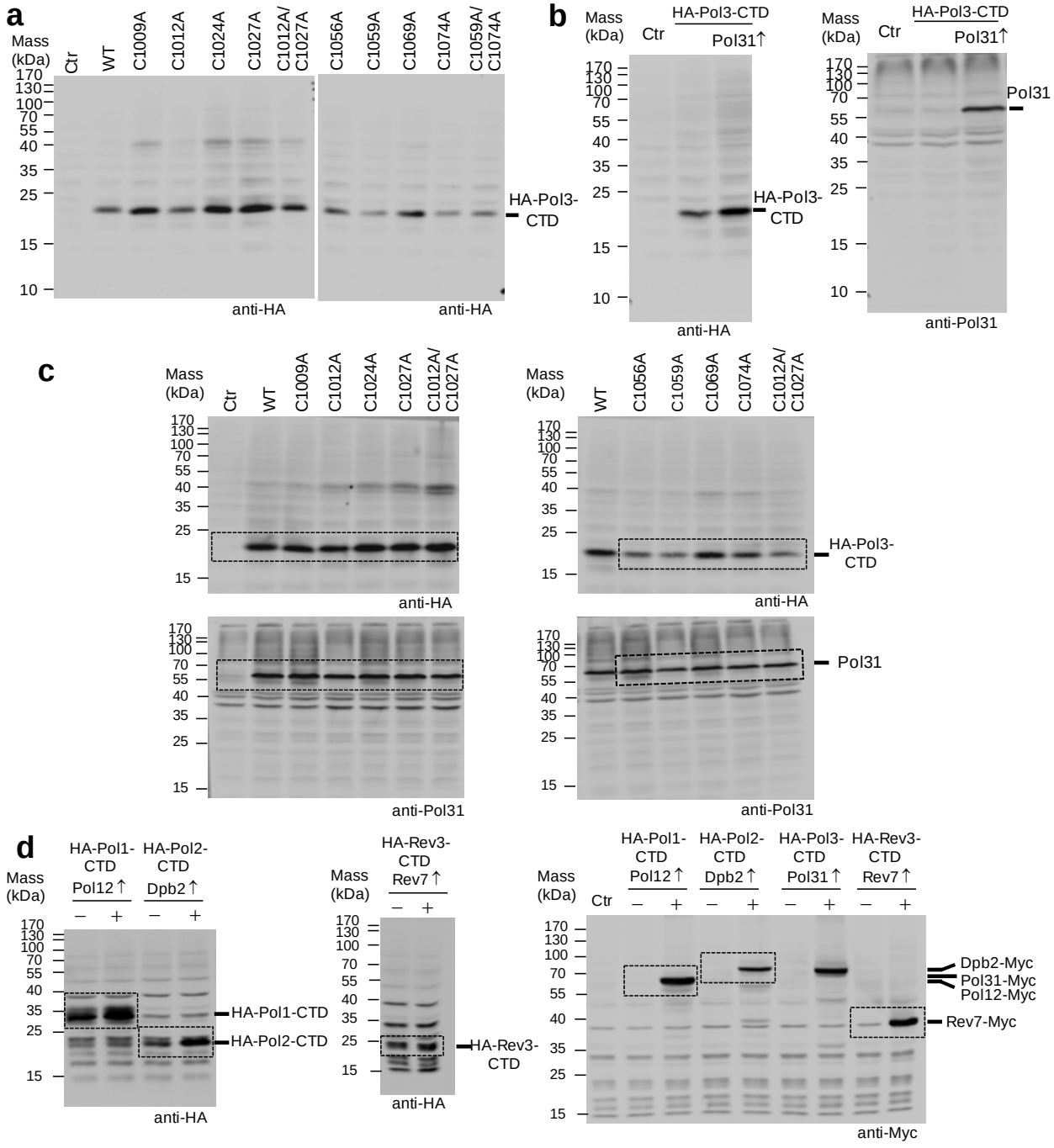

Supplementary Figure 8. Immunostaining for the Pol3-CTD ^{55}Fe incorporation experiment at endogenous Pol31 level and comparison of CTD and accessory subunit levels after over-expression. a, HA-Pol3-CTDs in cell extracts were visualized by immunostaining using specific antibodies and chemiluminescence detection by a CCD camera. Nomenclature corresponds to Fig. 2, samples are from the light olive-green bars in Fig. 2. **b,** Idem, but with comparison of HA-Pol3-CTD and Pol31 upon Pol31 over-expression (Pol31↑), **c, d** Full-size immunoblots corresponding to the cropped data (hatched boxes) shown in Figure 2a and 2b, respectively. The positions of molecular mass markers are indicated.

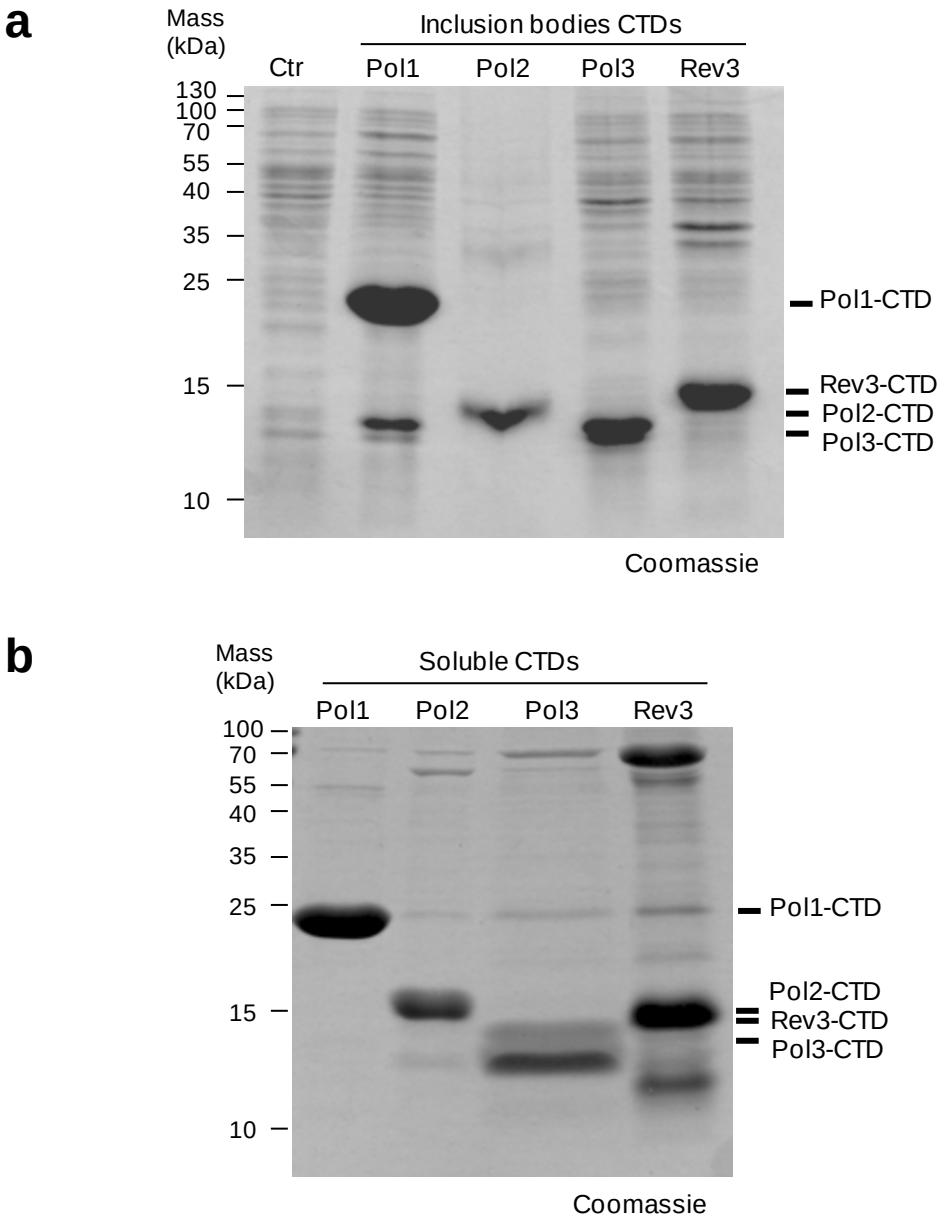

Supplementary Figure 9. Purification of DNA polymerase CTDs after expression in *E. coli*. a, Inclusion bodies solubilized with chaotropic agents (shown in Fig. 3a) were analyzed by SDS-PAGE and Coomassie staining. **b,** As in **a** but for soluble purified Pol1-, Pol2-, Pol3- and Rev3-CTDs used in Fig. 3 b,c and Supplementary Fig. 10.

Nature Chemical Biology: doi:10.1038/nchembio.721

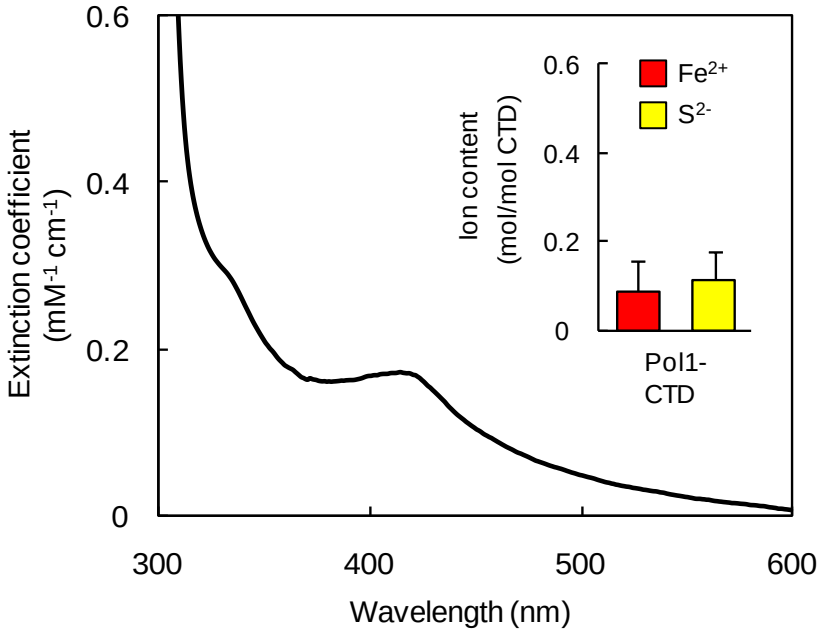

Supplementary Figure 10. UV-Vis spectrum of soluble purified Pol1-CTD. Pol1-CTD was purified as described in Methods. The inset shows the average non-heme iron and acid-labile sulfide content for three soluble Pol1-CTD preparations. Error bars, s.d. ($n \geq 3$).

Nature Chemical Biology: doi:10.1038/nchembio.721

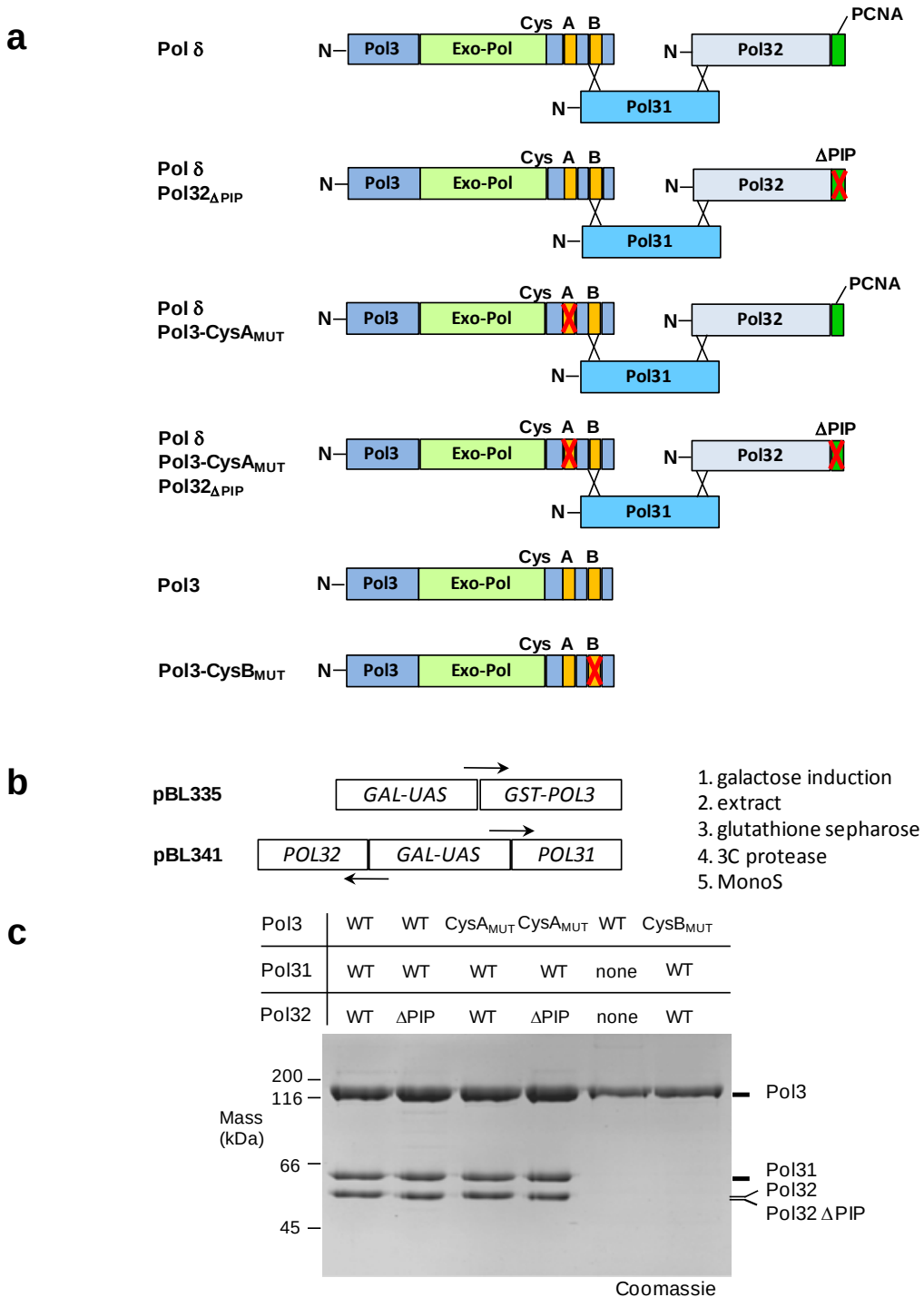

Supplementary Figure 11. Pol δ and Pol3 protein preparations used in this study. a, Overview of (mutant) Pol δ complexes used in Figs. 4 and 5. **b,** Scheme for overexpression (arrows indicate orientation of transcription) and protein purification. **c,** Photograph of the full length gel (SDS-PAGE) of purified proteins visualized by colloidal Coomassie staining. Fig. 4a in the main article contains cropped areas from the first, third and sixth lane of this gel image.

Nature Chemical Biology: doi:10.1038/nchembio.721

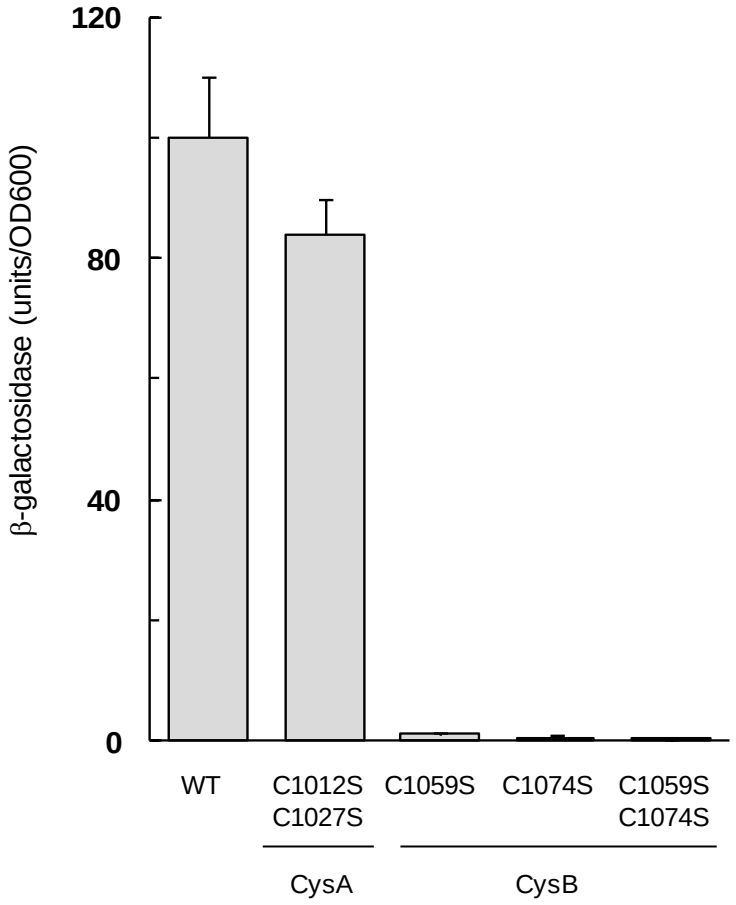

Supplementary Figure 12. Pol3-CysB mutants are defective in binding Pol31. Yeast two-hybrid interactions were measured employing plasmids with $LexA_{DBD}$-*POL3* (WT) or the indicated CysA and CysB mutants and with *GAL4*$_{AD}$-*POL31*. Averages of β-galactosidase activities are shown. Error bars, s.d. ($n \geq 3$).

Nature Chemical Biology: doi:10.1038/nchembio.721

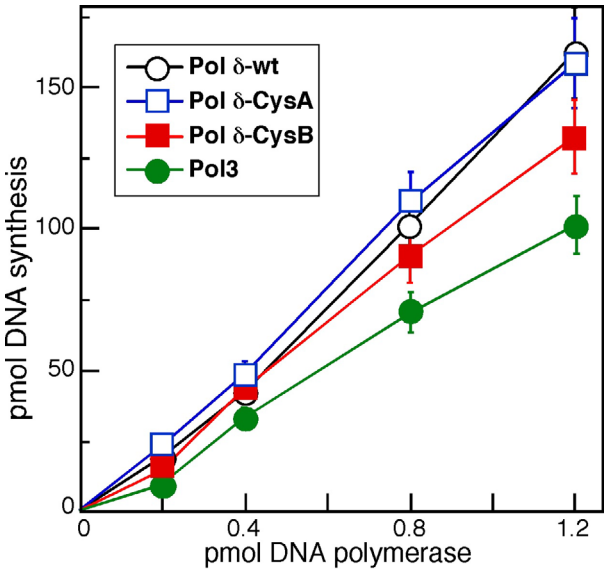

Supplementary Figure 13. Basal DNA polymerase activity of Pol δ is unaffected by CTD mutations. The assay measures incorporation of dNTPs into activated salmon sperm DNA as described[2]. Note that the activity of the single Pol3 enzyme (lacking Pol31 and Pol32) is somewhat lower. We ascribe this to its tendency to aggregation. Error bars, s.d. ($n \geq 3$).

Nature Chemical Biology: doi:10.1038/nchembio.721

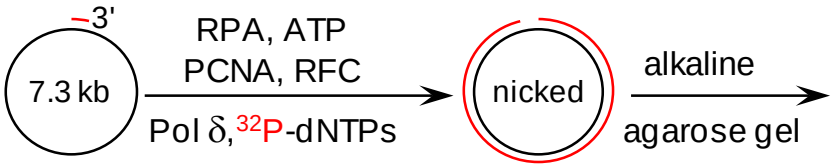

Supplementary Figure 14. Outline of the assay for processive DNA replication. The black circle represents single-stranded M13mp18 DNA primed with a 36 bp oligonucleotide (short red line) which is complementary to nucleotides 6330–6295. Polymerase replicates the single strand by extension of the primer with ^{32}P-dNTPs to form double-stranded DNA with a single nick. Formation of the radioactive strand (red) is subsequently detected by alkaline agarose gel electrophoresis and phosphorimaging (see Fig. 5 a and b).

Nature Chemical Biology: doi:10.1038/nchembio.721

Supplementary Table 1. **Yeast strains used in this study**.

Strain name	Background strain	Template for PCR (marker)	Tag and/or promoter introduced into genome	Source
Gal-NFS1	W303	pFA (His)	*GAL1-10* promoter	[3]
Gal-NBP35	W303	pFA (His)	*GAL1-10* promoter	[4]
Gal-NAR1	W303	pFA (His)	*GAL1-10* promoter	[5]
Pol1-Myc	W303	pYM19 (His)	C-terminal 9xMyc	this study
Pol2-Myc	W303	pYM19 (His)	C-terminal 9xMyc	this study
Pol3-Myc	W303	pYM21 (Nat)	C-terminal 9xMyc	this study
Rev3-Myc	W303	pYM19 (His)	C-terminal 9xMyc	this study
TFIIIA-Myc	Gal-NFS1	pYM21 (Nat)	C-terminal 9xMyc	this study
Gal-NFS1 Pol1-Myc	Pol1-Myc	pYM-N23 (Nat)	*GAL1-10* promoter	this study
Gal-NBP35 Pol1-Myc	Pol1-Myc	pYM-N23 (Nat)	*GAL1-10* promoter	this study
Gal-NFS1 Pol2-Myc	Pol2-Myc	pYM-N23 (Nat)	*GAL1-10* promoter	this study
Gal-NBP35 Pol2-Myc	Pol2-Myc	pYM-N23 (Nat)	*GAL1-10* promoter	this study
Gal-NFS1 Pol3-Myc	Gal-NFS1	pYM21 (Nat)	*GAL1-10* promoter	this study
Gal-NBP35 Pol3-Myc	Gal-NBP35	pYM21 (Nat)	*GAL1-10* promoter	this study
Gal-NAR1 Pol3-Myc	Gal-NAR1	pYM21 (Nat)	*GAL1-10* promoter	this study
GalL-HA-Pri2	W303	pYM-N28 (Nat)	*GALL* promoter & N-terminal 3xHA	this study
HA-Pri2	GalL-HA-Pri2	See text	Loss of *GALL* promoter	this study
HA-Pri2 Pol1-Myc	HA-Pri2	pYM21 (Nat)	C-terminal 9xMyc	this study

Abbreviations: pFA, pFA6a-HIS3MX6-Gal1-10; His, *Kluyveromyces lactis* His3; for pYM plasmids see[6]; Nat, nourseothricin acetyl transferase. TFIIIA is Transcription Factor IIIA (systematic name Pzf1).

Supplementary Table 2. **Plasmids used in this study.**

Plasmid (promoter)	Encoding protein	Tag and position		Use
416 (*MET25*)	Pol3-CTD	3HA	N	^{55}Fe incorporation
	Rev3-CTD	3HA	N	^{55}Fe incorporation
	Pol1-CTD	3HA	N	^{55}Fe incorporation
	Pol2-CTD	3HA	N	^{55}Fe incorporation
	Pol3-CTD C1009A	3HA	N	^{55}Fe incorporation
	Pol3-CTD C1012A	3HA	N	^{55}Fe incorporation
	Pol3-CTD C1024A	3HA	N	^{55}Fe incorporation
	Pol3-CTD C1027A	3HA	N	^{55}Fe incorporation
	Pol3-CTD C1012A/C1027A	3HA	N	^{55}Fe incorporation
	Pol3-CTD C1056A	3HA	N	^{55}Fe incorporation
	Pol3-CTD C1059A	3HA	N	^{55}Fe incorporation
	Pol3-CTD C1069A	3HA	N	^{55}Fe incorporation
	Pol3-CTD C1074A	3HA	N	^{55}Fe incorporation
	Pol3-CTD C1059A/C1074A	3HA	N	^{55}Fe incorporation
	ΔMTS-Nfs1	none		^{55}Fe incorporation
424 (*TDH*)	Pol12	3Myc	C	Co-expression with Pol1-CTD
	Dpb2	3Myc	C	Co-expression with Pol2-CTD
	Pol31	none		Co-expression with Pol3-CTD
	Rev7	3Myc	C	Co-expression with Rev3-CTD
pASK-IBA43plus (*TET*)	Pol1-CTD	Strep	C	Protein expression in *E.coli*
	Pol2-CTD	Strep	C	Protein expression in *E.coli*
	Pol3-CTD	Strep	C	Protein expression in *E.coli*
	Rev3-CTD	Strep	C	Protein expression in *E.coli*
pBL335 (*Gal1-10*)	GST-Pol3	GST	N	Protein expression in yeast
pBL341 (*Gal1-10*)	Pol31 and Pol32	none		Protein expression in yeast
pBL322 (*ADH*)	Pol3 (mutants)	$LexA_{DBD}$	N	Two-hybrid analysis
pBL364 (*ADH*)	Pol31	$GAL4_{AD}$	N	Two-hybrid analysis

Abbreviations: N, N-terminal; C, C-terminal; $LexA_{DBD}$, bacterial LexA DNA-binding domain; $GAL4_{AD}$, yeast *GAL4* activating domain. ΔMTS-Nfs1 is Nfs1 lacking amino acids 1-94[1].

Supplementary Methods

Yeast strains and genetic manipulation. Cassettes for the introduction of promoter sequences were amplified from pFA6a-HIS3MX6-Gal1-10[7], pYM-N23 or pYM-N27 templates[6]. pYM19 or pYM21 were used as template for C-terminal fusion of polymerase proteins with a nona-Myc tag sequence[6]. For these strains constructs the endogenous promoters remained unchanged. Exchange of the endogenous promoter for the *GalL* promoter with concomitant introduction of an N-terminal triple HA epitope tag for the construction of the GalL-HA-Pri2 strain was achieved with the pYM-N28 template[6]. Primers contained 20 nucleotides of the template plasmid and 50 nucleotides corresponding to the relevant genomic region used for homologous recombination. GalL-HA-Pri2 was converted to a strain with N-terminally tagged Pri2 under control of its natural promoter by homologous recombination and selection on glucose supplemented medium[8]. The fragment for recombination was obtained by PCR amplification of wild-type DNA with a promoter primer and the reverse complement of the 20 nucleotides directly 5' of the start ATG and 50 nucleotides encoding the HA tag. A complete list of strains and plasmids is presented in Supplementary Tables 1 and 2, respectively. Cells were grown in rich (YP) or minimal (SC) media at 30°C, containing the required carbon sources at a concentration of 2 % (w/v) and appropriate auxotrophic markers[9].

Cloning and cysteine mutagenesis of polymerase CTDs. A PCR fragment from pYM-N28[6] encoding an N-terminal triple HA tag was amplified with primers which added XbaI and SpeI restriction sites. The cut fragment was cloned into an XbaI-digested p416 plasmid with *Met25* promoter. Sequencing identified a clone with the correct orientation (p416-Met25-3HA). The coding regions of the CTDs of Pol3 (amino acids 982-1097), Rev3 (amino acids 1374-1504) Pol1, (amino acids 1262-1468) and Pol2 (amino acids 2084-2222) were PCR amplified from yeast chromosomal DNA with primers adding SpeI

Nature Chemical Biology: doi:10.1038/nchembio.721

(all) and EcoRI (Pol3 and Rev3) or HindIII (Pol1 and Pol2) restriction sites. After digestion, these fragments were cloned into the corresponding sites of p416-Met25-3HA. Pol3-CTD cysteine mutagenesis (see Supplementary Table 2 for plasmids) was carried out in p416-Met25-3HA-Pol3-CTD as template with primer design as described by Zheng et al.[10]. The Watcut tool (http://watcut.uwaterloo.ca/) from Michael Palmer (University of Waterloo, Canada) was used to introduce restriction sites with silent mutations. The coding regions of Pol31, Pol12, Dpb2 and Rev7 were PCR amplified from yeast chromosomal DNA with primers adding SpeI (all) and EcoRI (Pol31) or SalI (all other) restriction sites. After digestion, these fragments were cloned into the corresponding sites of p424-TDH (Pol31) or p424-TDH-3Myc (all other). The latter vector was prepared by cloning a fragment which was obtained by PCR amplification with primers adding SalI and XhoI restriction sites to the C-terminal 3Myc encoding region of pYM19[6] into p424-TDH.

Regions coding for the natural C terminus of the B-family polymerases were cloned into the NheI and NcoI restriction sites of pASK-IBA43-plus after amplification from yeast chromosomal DNA. This vector supplies a C-terminal Strep-tag. The constructs encompassed the following amino acids: Pol1, 1262-1468; Pol2, 2084-2222; Pol3, 982-1097 and Rev3, 1374-1504. All constructs and mutations were confirmed by DNA sequencing.

^{55}Fe incorporation into yeast proteins. The yeast strains listed in Supplementary Table 1 were grown in regular SC medium for 24 h, followed by growth in iron-free SC medium for 16 h. Depletion in glucose-containing medium led to less than 11 % decrease in cellular growth (wet cell mass) compared to wild-type cells. After washing with de-ionized water, cells (~0.5 g) were incubated for 2 h with $^{55}FeCl_3$ in iron-free SC medium. From this point onwards all steps were carried out below 4°C. Cells were collected by centrifugation and resuspended in an equal volume of TNETG buffer [10 mM Tris-

HCl pH 7.4, 150 mM NaCl, 2.5 mM EDTA, 0.5 % (v/v) Triton X-100, 10% (v/v) glycerol] with 2 mM PMSF and complete protease inhibitor tablets (Roche). Disruption of the cells was achieved by vortexing with glass beads in three one-min bursts, alternated with cooling on ice for 1 min. Cell debris were removed by centrifugation (1,500×*g*, 5 min), followed by clarification of the supernatant by centrifugation at 13,000×*g* for 12 min. Aliquots of 200 µl were incubated in 1.5 ml vials for 1 h with 20 µl suspension of agarose beads with coupled anti-Myc or anti-HA antibodies (Santa Cruz). After three washes with 0.5 ml TNTEG buffer, the beads were dispersed in 1 ml scintillation fluid and the amount of protein-associated ^{55}Fe was measured by scintillation counting (LS 6500, Beckman Coulter Inc.). Presence of tagged proteins and/or depletion of proteins in the cell extracts were confirmed by SDS-PAGE and immunostaining analysis of aliquots taken before immunoprecipitation. Monoclonal antibodies against Myc or HA epitopes were from Santa Cruz. Polyclonal antibodies against yeast Nfs1, Nbp35, Nar1, Porin, Pol31 and Pol32 proteins were raised in rabbits in our laboratories.

Yeast two-hybrid analysis. The interaction of the Pol3-CysB mutants with Pol31 was analyzed by yeast two-hybrid assays carried out in strain L40 (*MAT*a, *his3*-Δ*200*, *trp1-901*, *leu2-3,112*, *ade2*, *LYS2*::(lexAop)$_4$-*HIS3*, *URA3*::(lexAop)$_8$-lacZ) as described before[2]. Pol3-Pol31 interactions were measured using plasmid pBL322 (LexA$_{DBD}$-*POL3* in 2µ vector pBTM116 with *TRP1* marker) or its corresponding CysA (C1012S, C1027S) or CysB (C1059S, C1074S) mutants, and plasmid pBL364 (*GAL4*$_{AD}$-*POL31* in 2µ vector pACT2 with *LEU2* marker). Quantitative β-galactosidase assays were carried out in triplicate and were corrected for the background obtained in absence of the pBL364 plasmid.

Chemical analysis. Non-heme iron bound to protein was determined by colorimetry with the iron chelator Ferene[11]. Iron in (mutant) yeast Pol δ preparations was determined with the chelator 2-(5-nitro-2-pyridylazo)-5-(*N*-propyl-*N*-sulfopropylamine)phenol (nitro-PAPS)[12]. Quantitative release of iron ions from polymerase (25 µl) was effected by addition of 125 µl of 7 M guanidine hydrochloride, 0.4 M sodium acetate, 100 mM sodium thioglycolate at pH 4.3. After denaturation 75 µl water and 25 µl 1 mM nitro-PAPS were added. Spectra of the samples (200 µl) were recorded in flat bottom Greiner 96 well microtiter plates. The low pH value, wavelength (690 nm minus background at 900 nm) and presence of thioglycolate eliminated interference of other metal ions.

Acid-labile sulfide content was measured[11] by formation of methylene blue (absorbing at 670 nm) from the reaction of *N*,*N*'-dimethyl-*p*-phenylenediamine with H_2S and excess $FeCl_3$. Standardization was carried out with freshly purchased Li_2S. This method is highly specific for acid-labile sulfide and does not give a response with commonly encountered sulfur compounds including protein-bound cysteine or methionine[13]. The same method was downscaled 4-fold for determination of S^{2-} in microtiter plates (200 µl sample volume) and to confirm by visible spectroscopy that methylene blue was produced.

Protein concentrations for assays, Fe/S analysis and calculation of extinction coefficients were determined by the Bradford method, using bovine serum albumin as standard. The protein quantities were insufficient for extensive quantification with quantitative amino acid analysis or the biuret method. Metal and sulfide contents could therefore be influenced by small differences [~20 %][14] in the relative extent of color development of Pol δ and CTDs in comparison to the bovine serum albumin standard.

Statistical analysis. All quoted values have standard deviations (error bars in figures) calculated for at least three independent experiments. Significant means that values differ from the control or blank according to non-paired Student's t-test ($P < 0.05$).

Nature Chemical Biology: doi:10.1038/nchembio.721

References

1. Kispal, G., Csere, P., Prohl, C. & Lill, R. The mitochondrial proteins Atm1p and Nfs1p are required for biogenesis of cytosolic Fe/S proteins. *EMBO J.* **18**, 3981-3989 (1999).
2. Gerik, K. J., Li, X., Pautz, A. & Burgers, P. M. Characterization of the two small subunits of *Saccharomyces cerevisiae* DNA polymerase δ. *J. Biol. Chem.* **273**, 19747-19755 (1998).
3. Mühlenhoff, U. *et al.* Functional characterization of the eukaryotic cysteine desulfurase Nfs1p from *Saccharomyces cerevisiae*. *J. Biol. Chem.* **279**, 36906-36915 (2004).
4. Hausmann, A. *et al.* The eukaryotic P-loop NTPase Nbp35: An essential component of the cytosolic and nuclear iron-sulfur protein assembly machinery. *Proc. Natl. Acad. Sci. U.S.A.* **102**, 3266-3271 (2005).
5. Balk, J., Pierik, A. J., Netz, D. J. A., Mühlenhoff, U. & Lill, R. The hydrogenase-like Nar1p is essential for maturation of cytosolic and nuclear iron-sulphur proteins. *EMBO J.* **23**, 2105-2115 (2004).
6. Janke, C. *et al.* A versatile toolbox for PCR-based tagging of yeast genes: new fluorescent proteins, more markers and promoter substitution cassettes. *Yeast* **21**, 947-962 (2004).
7. Mühlenhoff, U., Richhardt, N., Ristow, M., Kispal, G. & Lill, R. The yeast frataxin homologue Yfh1p plays a specific role in the maturation of cellular Fe/S proteins. *Hum. Mol. Genet.* **11**, 2025-2036 (2002).
8. Booher, K. R. & Kaiser, P. A PCR-based strategy to generate yeast strains expressing endogenous levels of amino-terminal epitope-tagged proteins. *Biotechnol. J.* **3**, 524-529 (2008).
9. Sherman, F. Getting started with yeast. *Methods Enzymol.* **350**, 3-41 (2002).
10. Zheng, L., Baumann, U. & Reymond, J. L. An efficient one-step site-directed and site-saturation mutagenesis protocol. *Nucleic Acids Res.* **32**, e115 (2004).
11. Pierik, A. J. *et al.* Redox properties of the iron-sulfur clusters in activated Fe-hydrogenase from *Desulfovibrio vulgaris* (Hildenborough). *Eur. J. Biochem.* **209**, 63-72. (1992).
12. Makino, T., Kiyonaga, M. & Kina, K. A sensitive, direct colorimetric assay of serum iron using the chromogen, nitro-PAPS. *Clin. Chim. Acta* **171**, 19-27 (1988).
13. Rabinowitz, J. C. Analysis of acid-labile sulfide and sulfhydryl groups. *Methods Enzymol.* **53**, 275-277 (1978).
14. Peterson, G. L. Determination of total protein. *Methods Enzymol.* **91**, 95-119 (1983).

Nature Chemical Biology: doi:10.1038/nchembio.721